

RESEARCH

Open Access



Synthesis of novel mono- and bis-pyrazolylthiazole derivatives as anti-liver cancer agents through EGFR/HER2 target inhibition

Mostafa E. Salem¹, Esraa M. Mahrous¹, Eman A. Ragab¹, Mohamed S. Nafe² and Kamal M. Dawood^{1*} 

Abstract

3-Bromoacetyl-4-(2-naphthoyl)-1-phenyl-1H-pyrazole (6) was synthesized from 2-acetylnaphthalene and was used as a new key building block for constructing the title targets. Thus, the reaction of 6 with the thiosemicarbazones 7a–d and 9–11 afforded the corresponding simple naphthoyl-(3-pyrazolyl)thiazole hybrids 8a–d and 12–14. The symmetric bis-(2-naphthoyl-pyrazol-3-yl)thiazol-2-yl)hydrazono)methyl)phenoxy)alkanes 18a–c and 21a–c were similarly synthesized from reaction of 6 with the appropriate bis-thiosemicarbazones 17a–c and 19a–c, respectively. The synthesized two series of simple and symmetrical bis-molecular hybrid merging naphthalene, thiazole, and pyrazole were evaluated for their cytotoxicity. Compounds 18b,c and 21a showed the most potent cytotoxicity (IC_{50} = 0.97–3.57 μ M) compared to Lapatinib (IC_{50} = 7.45 μ M). Additionally, they were safe (non-cytotoxic) against the THLE2 cells with higher IC_{50} values. Compounds 18c exhibited promising EGFR and HER-2 inhibitory activities with IC_{50} = 4.98 and 9.85 nM, respectively, compared to Lapatinib (IC_{50} = 6.1 and 17.2 nM). Apoptosis investigation revealed that 18c significantly activated apoptotic cell death in HepG2 cells, increasing the death rate by 63.6-fold and arresting cell proliferation at the S-phase. Compound 18c upregulated P53 by 8.6-fold, Bax by 8.9-fold, caspase-3,8,9 by 9, 2.3, and 7.6-fold, while it inhibited the Bcl-2 expression by 0.34-fold. Thereby, compound 18c exhibited promising cytotoxicity against EGFR/HER2 inhibition against liver cancer.

Keywords EGFR/HER2, Liver cancer, Thiosemicarbazides bis-pyrazolylthiazoles, Naphthalenes

Introduction

Naphthalene ring is a great part of several significant biologically active synthetic and naturally-based organic compounds. It constitutes a distinguished core of various promising anti-cancer agents [1–7]. Some naturally

occurring naphthalene-based compounds, such as *Justicidin A*, and *Furomollugin* (Fig. 1), revealed outstanding anti-cancer activities [8, 9]. In addition, the naphthalene fragment was found in some commercially available marketed drugs such as *Naproxen* (anti-inflammatory drug), *Cinacalcet* (parathyroid carcinoma drug), *Terbinafine* (antifungal), *Nafcillin* (antibiotic), *Bedaquiline* (antitubercular), and *Nafimidone* (anticonvulsant) as shown in Fig. 1 [10, 11]. Interestingly, *Etalocib*, having 1,3-bis-phenoxypropane scaffold, was a drug candidate under phase trial III for the treatment of various types of cancer (Fig. 1) [12, 13]. Furthermore, many reviews reported the importance of thiazole-based heterocyclic compounds

*Correspondence:

Kamal M. Dawood
kmdawood@sci.cu.edu.eg

¹ Department of Chemistry, Faculty of Science, Cairo University, Giza 12613, Egypt

² Department of Chemistry (Biochemistry program), Faculty of Science, Suez Canal University, Ismailia 41522, Egypt



© The Author(s) 2023. **Open Access** This article is licensed under a Creative Commons Attribution 4.0 International License, which permits use, sharing, adaptation, distribution and reproduction in any medium or format, as long as you give appropriate credit to the original author(s) and the source, provide a link to the Creative Commons licence, and indicate if changes were made. The images or other third party material in this article are included in the article's Creative Commons licence, unless indicated otherwise in a credit line to the material. If material is not included in the article's Creative Commons licence and your intended use is not permitted by statutory regulation or exceeds the permitted use, you will need to obtain permission directly from the copyright holder. To view a copy of this licence, visit <http://creativecommons.org/licenses/by/4.0/>. The Creative Commons Public Domain Dedication waiver (<http://creativecommons.org/publicdomain/zero/1.0/>) applies to the data made available in this article, unless otherwise stated in a credit line to the data.

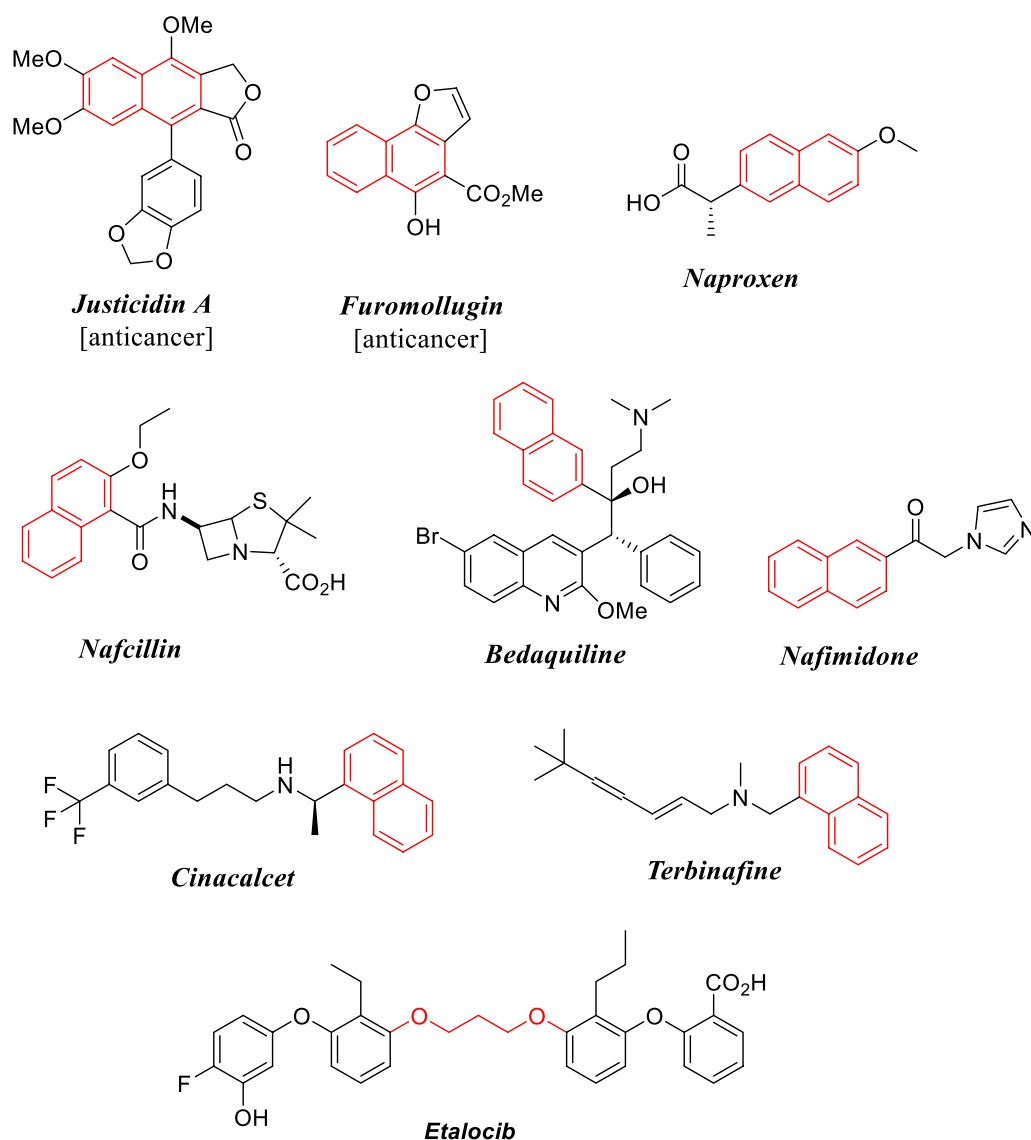


Fig. 1 Examples of naphthalene- and (bis-aryl)propylenedioxy-based marketed Drugs

as essential cores in several medicinally important compounds [14–18]. Thiazole nucleus is a fundamental part of some clinically applied anticancer drugs, such as *Tiazofurin* (1) [19], *Dasatinib* (2) [20], and *Dabrafenib* (3) [21] as depicted in Fig. 2.

In signal transduction pathways that control cell proliferation and differentiation, phosphotyrosine kinase, also known as receptor protein tyrosine kinase (RPTK), plays a crucial role. Transmembrane protein tyrosine kinase (PTK) epidermal growth factor receptor (EGFR) is a key regulator of cell proliferation, differentiation, and migration through ligand-induced dimerization [22]. The epidermal growth factor receptor (EGFR) tyrosine kinase-mediated cell growth signaling pathway

is involved in the initiation and progression of a wide variety of solid tumors, including those of the head and neck, lung, breast, bladder, prostate, and kidney [23]. As a result, EGFR tyrosine kinase is a promising therapeutic target. Over-expression or aberrant activation of EGFR and HER-2 is a major cause of cell malignant transformation, making them two of the most actively studied targets in oncology today [24]. The potentially useful new therapeutic anti-cancer drugs that block EGFR and/or HER-2 kinase activity upon ATP attachment to the receptor. For individuals with non-small-cell lung cancer, the US Food and Drug Administration (FDA) approved the inhibitors Gefitinib (Iressa) and Erlotinib (Tarceva) [25]. A synergistic anti-cancer effect may be displayed

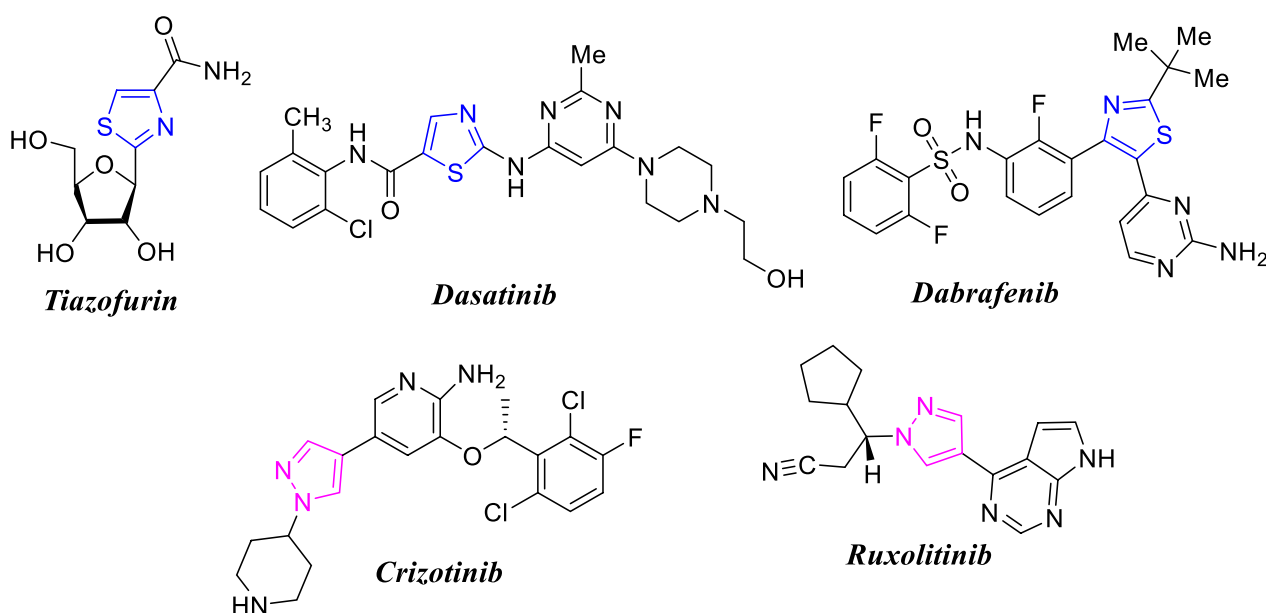


Fig. 2 Examples of thiazole- and pyrazole-based anti-cancer drugs

by the pyrazole ring in conjunction with the thiazole and naphthalene rings in the combined substructures [26].

Besides, pyrazole moiety is one of the most predominant classes of nitrogen heterocycles that are widely found in a huge number of synthetic and naturally occurring organic compounds that possess significant anti-cancer activity [27–29]. Interestingly, some pyrazole scaffolds were also approved by FDA as commercially available anti-cancer drugs, such as *Crizotinib* [for treatment of non-small cell lung carcinoma (NSCLC)] [30, 31], and *Ruxolitinib* (for treatment of myelofibrosis) [32] (Fig. 2).

Merging two or more aryl(heteroaryl) fragments in one molecule to construct a new hybrid molecule is a beneficial tool for the designing of effective therapeutic agents [33, 34]. In this regard, some naphthyl-pyrazole hybrids **A–E** demonstrated potent in vitro anti-cancer efficiency against human breast cancer cell line MCF-7 (Fig. 3) [35–38]. Interestingly, some of these derivatives exhibited high anti-cancer activity against MCF-7 with a five-fold more active than the reference drug cisplatin [37]. In addition, some molecules involving the three scaffolds; pyrazole, thiazole, and naphthalene, were reported to have notable anti-cancer activity targeting EGFR (Fig. 3) [39, 40].

Recently, our research was directed towards synthesis of variant simple and bis-heterocyclic hybrids having significant anti-cancer potency against several human cancer cell lines [41–51]. Inspired by the observations mentioned above, herein we designed and synthesized a new series of molecular hybrids merging the three

fragments: naphthalene, thiazole, and pyrazole, in addition to benzothiazole, benzofuran or coumarin in a simple- and symmetrical bis-molecularly hybrid forms aiming at the production of more efficient anti-cancer hybrid structures (Fig. 4).

Results and discussion

Chemistry

A sequence of processes, as described in Scheme 1, was used to produce the desired key building block; 3-bromoacetyl-4-(2-naphthoyl)-1-phenyl-1H-pyrazole (**6**). Thus, 2-acetylnaphthalene (**1**) was refluxed with dimethylformamide-dimethylacetal (DMF-DMA) to give 3-(dimethylamino)-1-(naphthalen-2-yl)prop-2-en-1-one (**3**). Treatment of the latter enaminone **3** with 2-oxo-*N*²-phenylpropanehydrazonoyl chloride (**4**) in refluxing benzene in the presence of triethylamine produced 3-acetyl-4-(2-naphthoyl)-1-phenyl-1H-pyrazole (**5**) in a good yield. Bromination of the latter 3-acetylpyrazole **5** with bromine in acetic acid at 80–90 °C furnished the corresponding new 3-bromoacetylpyrazole derivative **6** in 78% yield (Scheme 1). The structures of the *hitherto* unreported naphthoylpyrazoles **5** and **6** were inferred from their elemental and spectral analyses, as described in the experimental section.

The reaction of 3-bromoacetylpyrazole derivative **6** with the appropriate aldehyde-thiosemicarbazone derivatives **7a–d** in refluxing ethanol in the presence of few drops of triethylamine afforded the corresponding new 2-(benzylidenehydrazinyl)-4-(pyrazol-3-yl)thiazole derivatives **8a–d** (Scheme 2). The structures of the

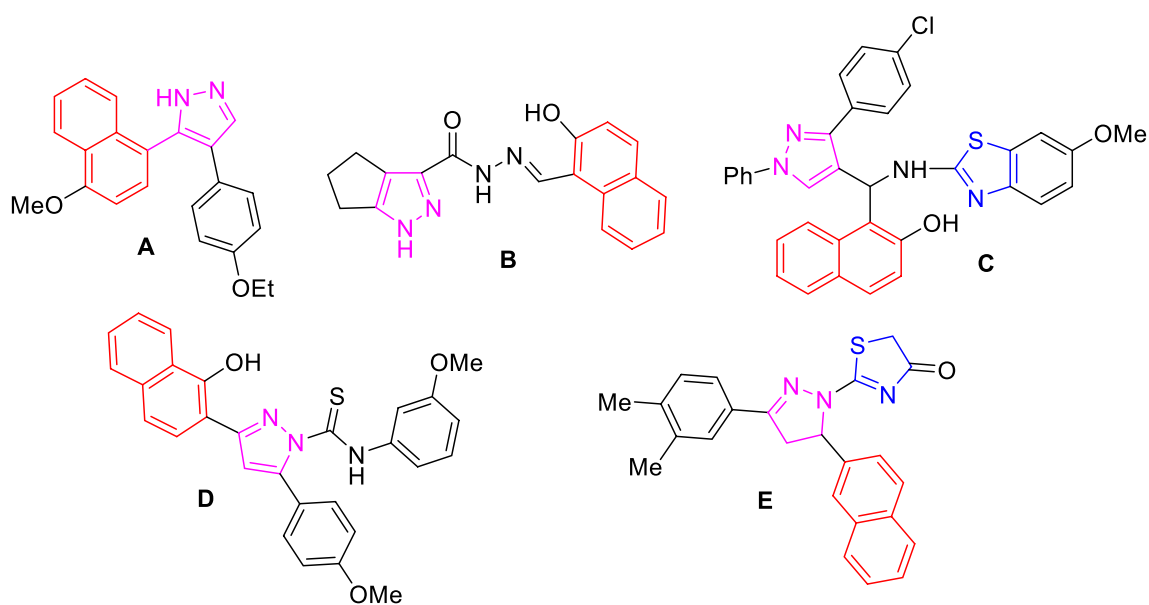


Fig. 3 Anti-cancer molecular hybrids **A-E** have pyrazole, thiazole, and naphthalene moieties

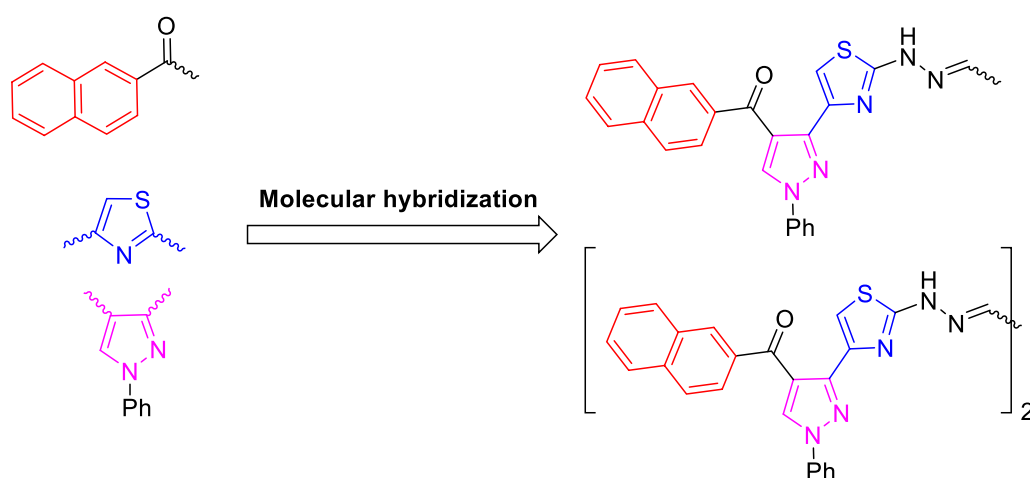
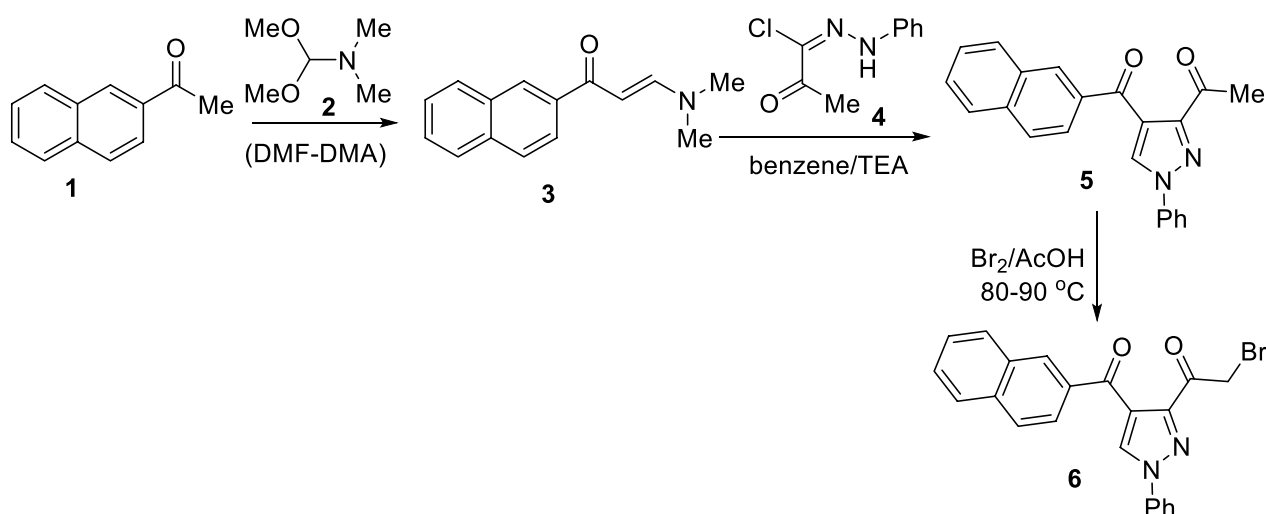


Fig. 4 Rationale Design for molecular hybridization towards new anti-cancer agents

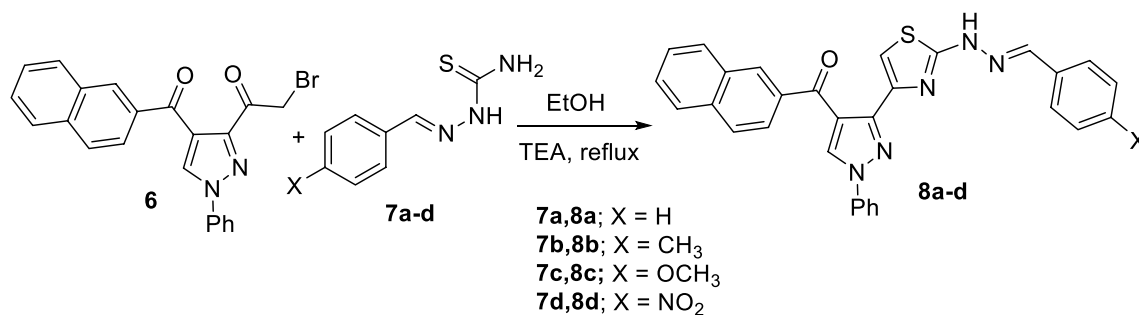
obtained products were substantiated from their elemental and spectral analyses. The $^1\text{H-NMR}$ of compound **8a**, as a demonstrative example, showed five singlet signals at 7.95, 8.06, 8.51, 9.02 and 12.09 due to the thiazole-5-CH, CH=N, naphthyl-1-CH, pyrazole-5-CH, and NH protons, respectively. The $^{13}\text{C-NMR}$ of **8a** revealed 25 signals due to 25 different sp^2 carbons. Its IR showed two distinctive absorption peaks at 3437 and 1647 due to NH and C=O functions. In addition, its mass spectrometry exhibited a peak at m/z 499 due to its molecular ion.

Similarly, reaction of the 3-bromoacetylpyrazole derivative **6** with three different heterocycl-thiosemicarbazones **9**, **10**, and **11**, under similar reaction conditions as

mentioned above, yielded the corresponding 4-(3-pyrazolyl)thiazole derivatives **12**~**14** having benzofuran, benzothiazole, and coumarin moieties, in 85%, 87%, and 73% yields, respectively (Scheme 3). Compounds **12**~**14** represent fascinating hybrid compounds that each has a different bioactive heterocyclic moiety. The structures of compounds **12**~**14** were established from their elemental analyses and spectral data. The $^1\text{H-NMR}$ spectrum of compound **12** revealed six singlet signals at 2.31, 7.22, 7.89, 8.55, 9.04, and 11.59 due to the methyl, benzofuran-3-H, thiazole-5-CH, naphthyl-1-CH, pyrazole-5-CH, and NH protons, respectively. Its IR showed two distinctive absorption peaks at 3433 and 1648 due to NH and C=O



Scheme 1 Synthesis of 3-bromoacetyl-4-(2-naphthoyl)-1-phenyl-1H-pyrazole (**6**)



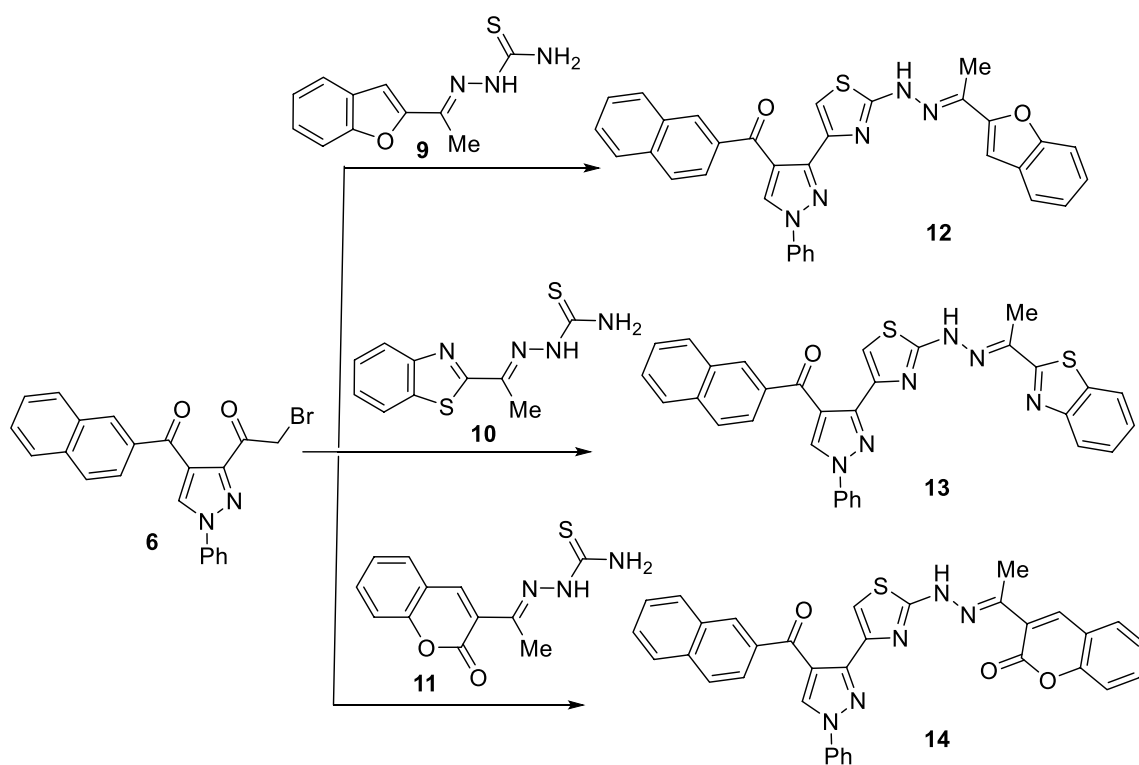
Scheme 2 Synthesis of 2-(arylidenehydrazinyl)-4-(3-pyrazolyl)thiazole derivatives **8a-d**

functions. In addition, its mass spectrometry exhibited a peak at m/z 533 due to the molecular ion.

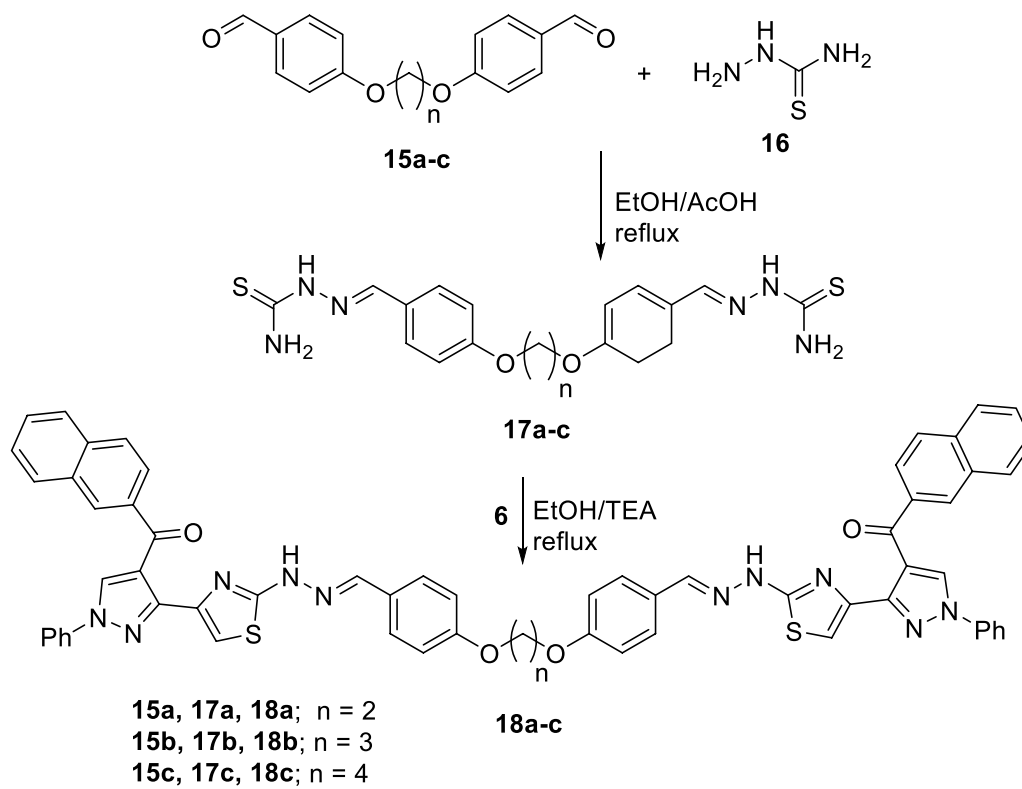
Next, we intended to construct symmetric *bis*-heterocyclic systems to compare their behaviors with the mono-heterocyclic systems that were described in the above text. Thus, two series of *bis*-pyrazolylthiazoles linked via alkyleneoxy-phenylene spacers at either *ortho*- or *para*-positions were developed. Firstly, the starting building blocks **17a-c** and **20a-c** were prepared according to methodologies reported in the literature via reaction of the appropriate *bis*(aldehydes) **15a-c** and **19a-c** with thiosemicarbazid **16** in refluxing ethanol containing few drops of acetic acid (Schemes 4 and 5). Then, the synthesis of 1,2-bis(4-((2-(4-((2-naphthoyl)-1-phenyl-1H-pyrazol-3-yl)thiazol-2-yl)hydrazono)methyl)phenoxy)ethane (**18a**) was achieved by the reaction of 3-(bromoacetyl)-4-(2-naphthoyl)-1-phenyl-1H-pyrazole (**6**) with 4,4'-(ethane-1,2-diylbis(oxy))dibenzaldehyde-thiosemicarbazone (**17a**) in ethanol, in the presence of few drops of triethylamine, at reflux temperature. The

bis-pyrazolylthiazole derivative **18a** was isolated in a 79% yield (Scheme 4). Further examples; the symmetric bis(4-((2-(4-((2-naphthoyl)-1-phenyl-1H-pyrazol-3-yl)thiazol-2-yl)hydrazono)methyl)phenoxy)alkanes **18b,c** were similarly synthesized under typical reaction condition from the reaction of the bromoacetylpyrazole **6** with the appropriate 4,4'-(alkane-diylbis(oxy))dibenzaldehydethiosemicarbazone derivatives **17b,c**. The symmetric *bis*-pyrazolylthiazoles **18b,c** were obtained in 80 and 83% yields, respectively (Scheme 4). The $^1\text{H-NMR}$ spectrum of compound **18a** displayed six singlet signals at 4.35, 7.91, 8.06, 8.51, 9.01 and 11.90 due to the CH_2O , thiazole-5-CH, $\text{CH}=\text{N}$, naphthyl-1-CH, pyrazole-5-CH, and NH protons, respectively. The $^{13}\text{C-NMR}$ spectrum of compound **18a** exhibited a signal at 65.4 due to an sp^3 CH_2O carbon in addition to 26 signals due to 26 different sp^2 carbons. The IR spectrum of compound **18a** showed two absorption bands at 3407 and 1645 cm^{-1} due to NH and $\text{C}=\text{O}$ functions (Additional file 1).

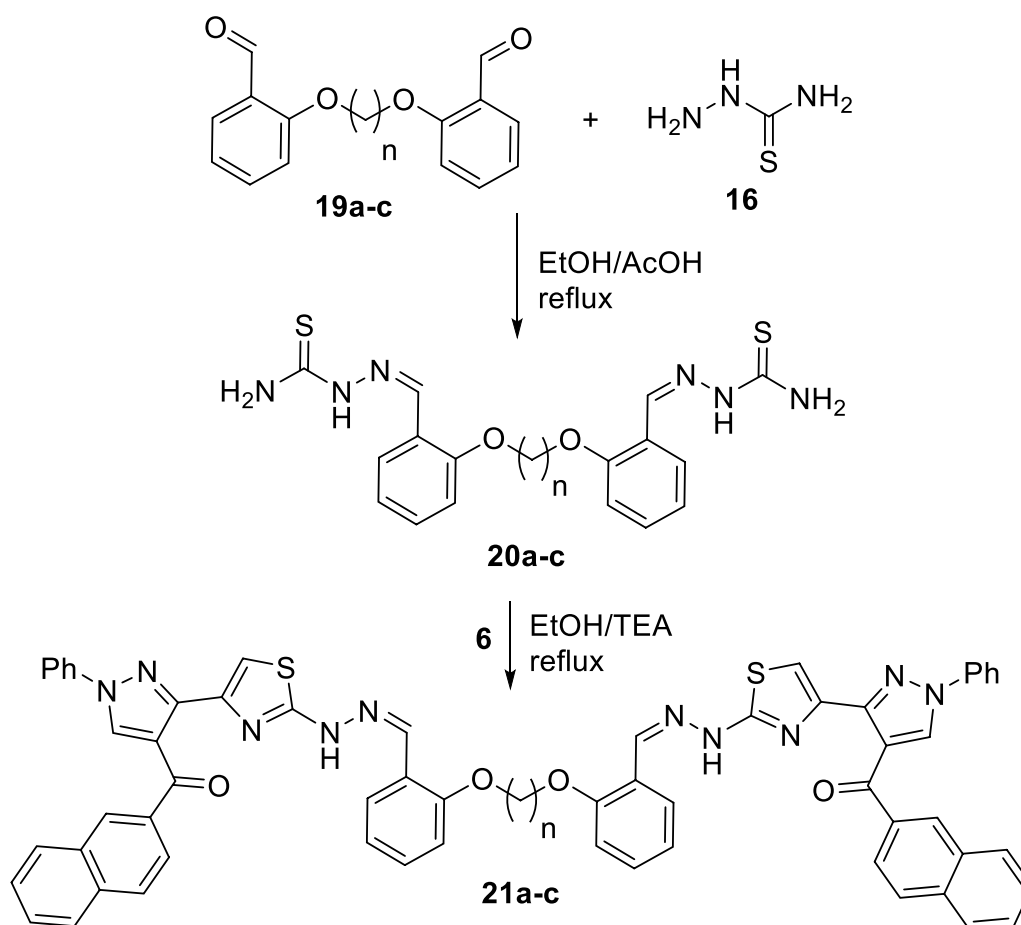
Similarly, the 2,2'-(alkane-diylbis(oxy))dibenzaldehydethiosemicarbazone derivatives **19a-c** reacted with



Scheme 3 Synthesis of arylidenehydrazinyl-(1H-pyrazol-3-yl)thiazole derivatives **12–14**



Scheme 4 Reaction of bis(thiosemicarbazones) **17a–c** with bromoacetylpyrazole **6**



19a, 20a, 21a; $n = 2$

19b, 20b, 21b; $n = 3$

19c, 20c, 21c; $n = 4$

Scheme 5 Reaction of bis(thiosemicarbazones) **20a–c** with bromoacetylpyrazole **6**

the bromoacetylpyrazole **6**, under typical reaction conditions as above to give the corresponding bis(2-((2-(4-((2-naphthoyl)-1-phenyl-1H-pyrazol-3-yl)thiazol-2-yl)hydrazono)-methyl)phenoxy)alkanes **21a–c** (*ortho* isomers) in 70–78% yields, as shown in Scheme 5. The structures of the pure products were established from their respective elemental and spectral analyses, as described in the experimental section. For instance, the ^1H NMR spectrum of **21a** showed a D_2O -exchangeable signal at 11.95 ppm assigned to NH protons as well as a sharp singlet signal at δ 8.29 due to a methine proton ($\text{N}=\text{CH}$). Moreover, it also featured a singlet signal at δ 4.40 due to methylene ether linkage OCH_2 .

Biology

Cytotoxicity

The synthesized compounds were screened for their cytotoxicity against HepG2 cells using the MTT assay. As seen in Table 1, the bis-pharmacophores exhibited much higher cytotoxicity than the mono-pharmacophoric compounds. Fourteen substrates were tested for their anti-cancer activity. Among them, eight compounds (**8c**, **12**, **13**, **14**, **18b,c**, **21a,c**) were found to have high anti-cancer potency with IC_{50} values ranging between 0.97–7.39 μM much better than the reference drug Lapatinib ($\text{IC}_{50}=7.45 \mu\text{M}$). The order of anti-cancer potency of the tested compounds was arranged in the following order: **18c** > **21a** > **18b** > **21c** > **14** > **13** > **12** > **8c**. Interestingly, compounds **18c**, **21a**, and **18b** showed potent

Table 1 Cytotoxic IC₅₀ values of the tested compounds against HepG2 and THLE2 cell lines using the MTT assay

Compounds	IC ₅₀ ± SD ^a (μM)	
	HepG2	THLE2
6	16.3 ± 0.29	34.5 ± 1.26
8a	8.64 ± 0.29	46.2 ± 2.01
8b	8.16 ± 0.34	41.6 ± 1.86
8c	7.39 ± 0.29	≥ 50
8d	11.3 ± 0.34	≥ 50
12	5.48 ± 0.66	≥ 50
13	5.16 ± 0.29	≥ 50
14	4.36 ± 0.38	39.5 ± 1.74
18a	8.34 ± 0.48	39.8 ± 1.59
18b	3.57 ± 0.67	≥ 50
18c	0.97 ± 0.09	≥ 50
21a	3.26 ± 0.14	≥ 50
21b	9.36 ± 0.47	49.4 ± 2.1
21c	4.12 ± 0.19	45.6 ± 1.87
Lapatinib	7.45 ± 0.32	≥ 50

^a Values are expressed as Mean ± SD of three independent triplets (n = 3)

cytotoxicity with IC₅₀ values of 0.97, 3.26 and 3.57 μM, respectively, compared with the reference anti-cancer drug Lapatinib (IC₅₀ = 7.45 μM). These compounds caused cell viability at the highest concentration [100 μM] by 5%, 13%, and 9%, respectively, as shown in Fig. 5. Additionally, they were safe (non-cytotoxic) against the THLE2 cells with higher IC₅₀ values. Among the mono-pharmacophoric compounds **8a-d**, the best activity was recorded for the benzaldehyde-hydrazone derivative **8c** having para-methoxy group. For comparison reasons, the activity of the bis-pyrazolylthiazole pharmacophores connected via para-alkanedioxy or ortho-alkanedioxy linkers **18a-c** and **21a-c** were compared with the simple pyrazolylthiazole having para-methoxybenzaldehyde hydrazine **8c**. Interestingly, doubling the pharmacophoric scaffold led to about eightfold enhancement in the anti-cancer potency (IC₅₀ = 0.97 μM for **18c** vs. 7.39 μM for **8c**), as presented in Fig. 6. In addition, the mono-pyrazolylthiazole derivatives having acetyl-heterocyclic-hydrazones **12~14** (benzofuranyl, benzothiazolyl and coumarinyl) were more potent against HepG2 cell line than those having aryl moieties **8a-d**.

EGFR and HER2 kinase inhibitory assay

Compounds **18c**, **21a**, and **18b** with the highest cytotoxic activity against HepG2 cells were tested against the EGFR/HER2 inhibitory activities to highlight their mechanistic study. As seen in Table 2, the tested compounds exhibited promising dual EGFR/HER2 inhibition activities. Interestingly, compound **18c** had IC₅₀ values

of 4.98 and 9.85 nM, respectively compared to Lapatinib (IC₅₀ = 6.1 and 17.2 nM). Additionally, compounds **21a** and **18b** exhibited promising EGFR/HER2 inhibition with IC₅₀ values of 5.8, 7.04 nM against EGFR and 14.2, 16.3 nM against HER2. Hence, compound **18c** was further investigated for apoptotic cell death in HepG2 cells. These findings agreed with previous studies [52–54] about hybrid structures having pyrazole and thiazole rings, revealing that the two combined moieties might exhibit synergistic anti-cancer effects as potential EGFR and HER-2 inhibitory agents.

Apoptotic investigation

Annexin V/PI staining with cell cycle analysis The apoptotic activity of compound **18c** (IC₅₀ = 0.97 M, 48 h) was evaluated by comparing the percentage of dead cells in untreated and treated HepG2 cells using flow cytometry after staining with Annexin V and PI. As shown in Fig. 7A, compound **18c** significantly activated apoptotic cell death in HepG2 cells, increasing the death rate by 63.6-fold; it induced total apoptosis by 41.35% (15.28% for early apoptosis, 26.07% for late apoptosis) compared to the untreated control group (0.65%).

Afterward, DNA flow cytometry was used to determine the cell population in each cell phase following treatment with a cytotoxic agent. As seen in Fig. 7B, compound **18c** treatment significantly increased cells at the S-phase by 50.5% compared to control 37.8%, while cells in G0-G1 were not significantly increased, and cells in G2/M were decreased. Consequently, compound **18c** induced apoptosis in HepG2 cells arresting the cell proliferation at S-phase.

RT-PCR For validating the apoptotic cell death in HepG2 cells upon treatment with compound **18c**, gene expression level using RT-PCR was investigated for the apoptosis-mediated genes of P53, Bax, caspase-3,8,9 and Bcl-2 in both untreated and treated HepG2 cells. As seen in Fig. 8, compound **18c**, upregulated P53 by 8.6-fold, Bax by 8.9-fold, caspase-3,8,9 by 9, 2.3, and 7.6-fold, while it inhibited the Bcl-2 expression by 0.34-fold. Therefore, our results demonstrated that the intrinsic mechanism of apoptosis was responsible for the cell death induced by treatment with compound **18c**. Caspases are involved in both the beginning and end of the death process in mitochondria-mediated apoptosis. Loss of mitochondrial potential can be triggered by upregulating proapoptotic subunits over antiapoptotic proteins like Bcl-2 protein. By increasing proapoptotic proteins and decreasing antiapoptotic proteins, the intrinsic apoptotic pathway is activated, and mitochondria lose their mitochondrial potential (ΔΨ_m), releasing cytochrome c, which triggered caspase 3 and 9

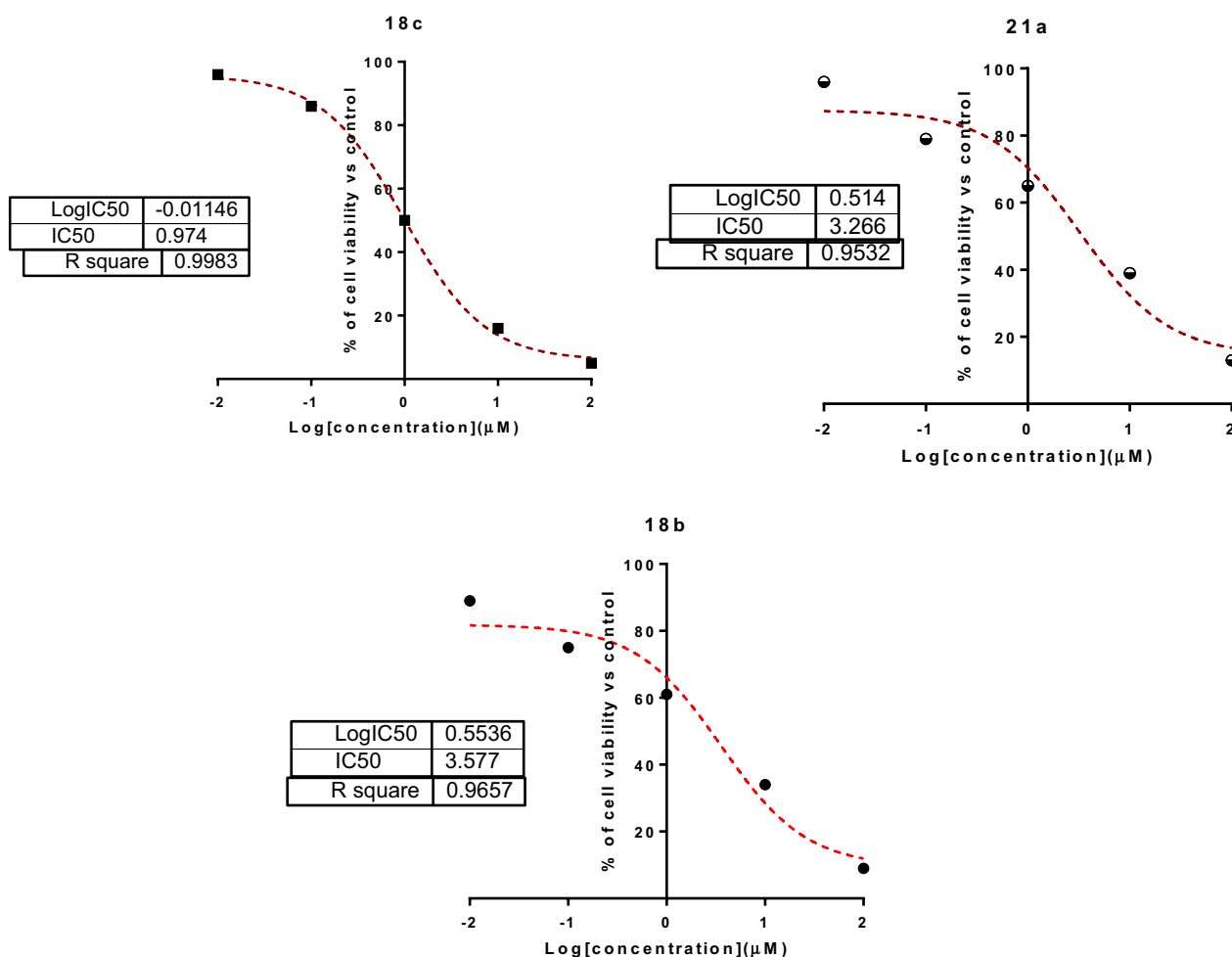


Fig. 5 The current most potent anti-cancer mono- and bis-pharmacophores

activations and, ultimately, cell death via caspase-dependent apoptosis.

Experimental section

Chemistry

Melting points were determined in open glass capillaries with a Gallenkamp apparatus. Elemental analyses were carried out at the Microanalytical Center of Cairo University, Giza, Egypt. The infrared spectra were recorded as potassium bromide disks on a Pye Unicam SP 3–300 and Shimadzu FTIR 8101 PC infrared spectrophotometer. NMR spectra were recorded on Varian Mercury VXR-300 NMR spectrometer at 300 MHz (^1H NMR) and at 75 MHz (^{13}C NMR) using $\text{DMSO-}d_6$ as solvent. Chemical shifts were reported downfield from TMS ($=0$) for ^1H NMR. For ^{13}C NMR, chemical shifts were reported in the scale relative to the solvent used as an internal reference. Mass spectra (EI) were obtained at 70 eV with a type Shimadzu GCMQP 1000 EX spectrometer. The enaminone **3**, [55] hydrazoneyl chloride **4**, [56]

aldehyde-thiosemicarbazones **7a-c**, [57, 58] acetyl-thiosemicarbazones **9**, **10**, **11** [59, 60], bis-aldehydes **15a-c**, **19a-c** [61–63], and bis-thiosemicarbazones **17a-c**, **20a-c**, [64–67] were prepared following procedures reported in the literature.

Synthesis of benzylidenehydrazinyl-(1H-pyrazol-3-yl)thiazole derivatives **8a-d**

General procedure To a mixture of 3-bromoacetyl-4-(2-naphthoyl)-1-phenyl-1H-pyrazole (**6**) (1.0 mmol) and the appropriate aldehyde-thiosemicarbazone derivatives **7a-d** (1.0 mmol) in ethanol (20 mL), triethylamine (0.2 mL) were added, and the mixture was heated under reflux for 3–5 h. The reaction mixture was allowed to cool to room temperature, and the solvent was evaporated under vacuum. The solid residue was collected by filtration and recrystallized from ethanol/DMF to give the corresponding 2-(benzylidenehydrazinyl)-4-(pyrazol-3-yl)thiazole derivatives **8a-d**.

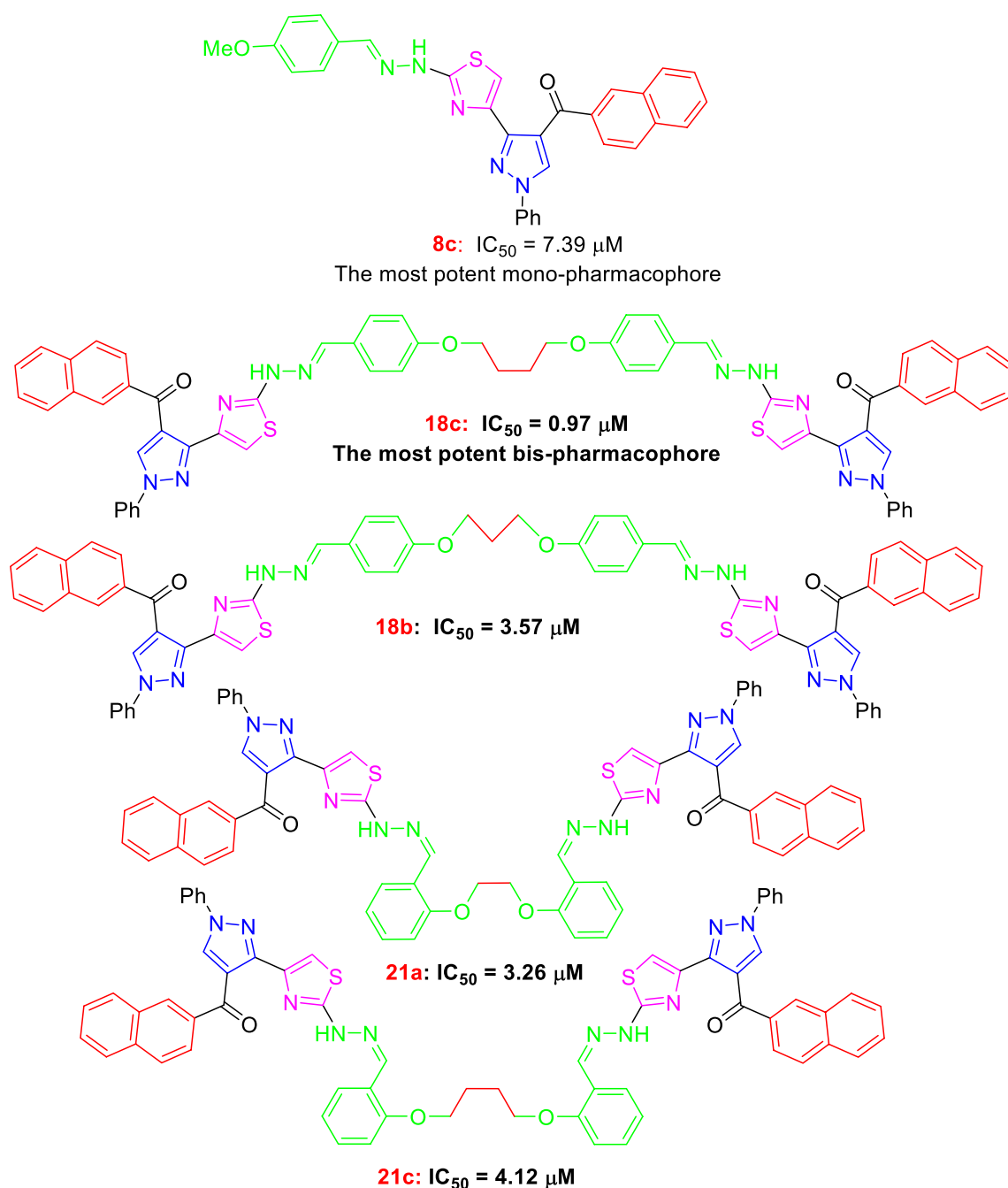


Fig. 6 Dose–response nonlinear regression curve fitting the percentage of cell viability vs. log [conc. μM], R square ≈ 1 using the GraphPad prism

2-(Benzylidenehydrazinyl)-4-(4-(2-naphthoyl)-1-phenyl-pyrazol-3-yl)thiazole (8a)

Yellow crystals, (88% yield), mp. 138–140 °C; IR (KBr) 3437 (NH), 1647 (C=O), 1576 (C=N) cm^{-1} ; 1H -NMR δ 7.35–7.66 (m, 11H, ArH), 7.95 (s, 1H, thiazole-5-H), 7.98–8.03 (m, 3H, ArH), 8.06 (s, 1H, CH=N), 8.12 (d, 2H, ArH, $J=7.8$), 8.51 (s, 1H, naphthalene-1-H), 9.02 (s,

1H, pyrazole-5-H), 12.09 (s, 1H, NH); ^{13}C NMR: δ 108.4, 119.0, 120.9, 124.7, 126.2, 126.8, 127.1, 127.6, 128.2, 128.5, 128.8, 129.2, 129.6, 129.8, 131.6, 132.1, 132.7, 134.3, 134.9, 135.7, 138.9, 141.1, 147.9, 167.6, 189.0; MS: m/z 499 (M^+). Anal. Calcd. for $C_{30}H_{21}N_5OS$: C, 72.12; H, 4.24; N, 14.02; S, 6.42. Found: C, 72.10; H, 4.22; N, 14.03; S, 6.39%.

Table 2 IC₅₀ values of EGFR and HER2 kinase activities of the most potent compounds

Compound	IC ₅₀ [nM] ^a	
	EGFR kinase	HER2 kinase
18b	7.04	16.3
18c	4.98	9.85
21a	5.8	14.2
Lapatinib	6.1	17.2

^a Values are expressed as an average of three independent replicates. IC₅₀ values were calculated using a sigmoidal non-linear regression curve fit of percentage inhibition against five concentrations of each compound

2-(4-Methylbenzylidenehydrazinyl)-4-(4-(2-naphthoyl)-1-phenylpyrazol-3-yl)thiazole (8b)

Brown powder, (83% yield), mp. 207–210 °C; IR (KBr) 3432 (NH), 1648 (C=O), 1578 (C=N) cm⁻¹; ¹H-NMR: δ 2.31 (s, 3H, CH₃), 7.21 (d, 2H, ArH, *J*=7.8), 7.37–7.68 (m, 8H, ArH), 7.91 (s, 1H, thiazole-5-H), 7.96–8.03 (m, 3H, ArH), 8.06 (s, 1H, CH=N), 8.12 (d, 2H, ArH, *J*=8.1), 8.51 (s, 1H, naphthalene-1-H), 9.01 (s, 1H, pyrazole-5-H), 11.96 (s, 1H, NH); ¹³C NMR: δ 23.4, 102.5, 114.9, 115.7, 116.1, 118.3, 121.1, 127.3, 128.4, 128.5, 128.6, 128.7, 128.8, 129.0, 129.2, 130.1, 130.5, 130.8, 131.1, 131.5, 135.5, 136.1, 138.1, 141.1, 147.9, 169.2, 191.1. MS: *m/z*

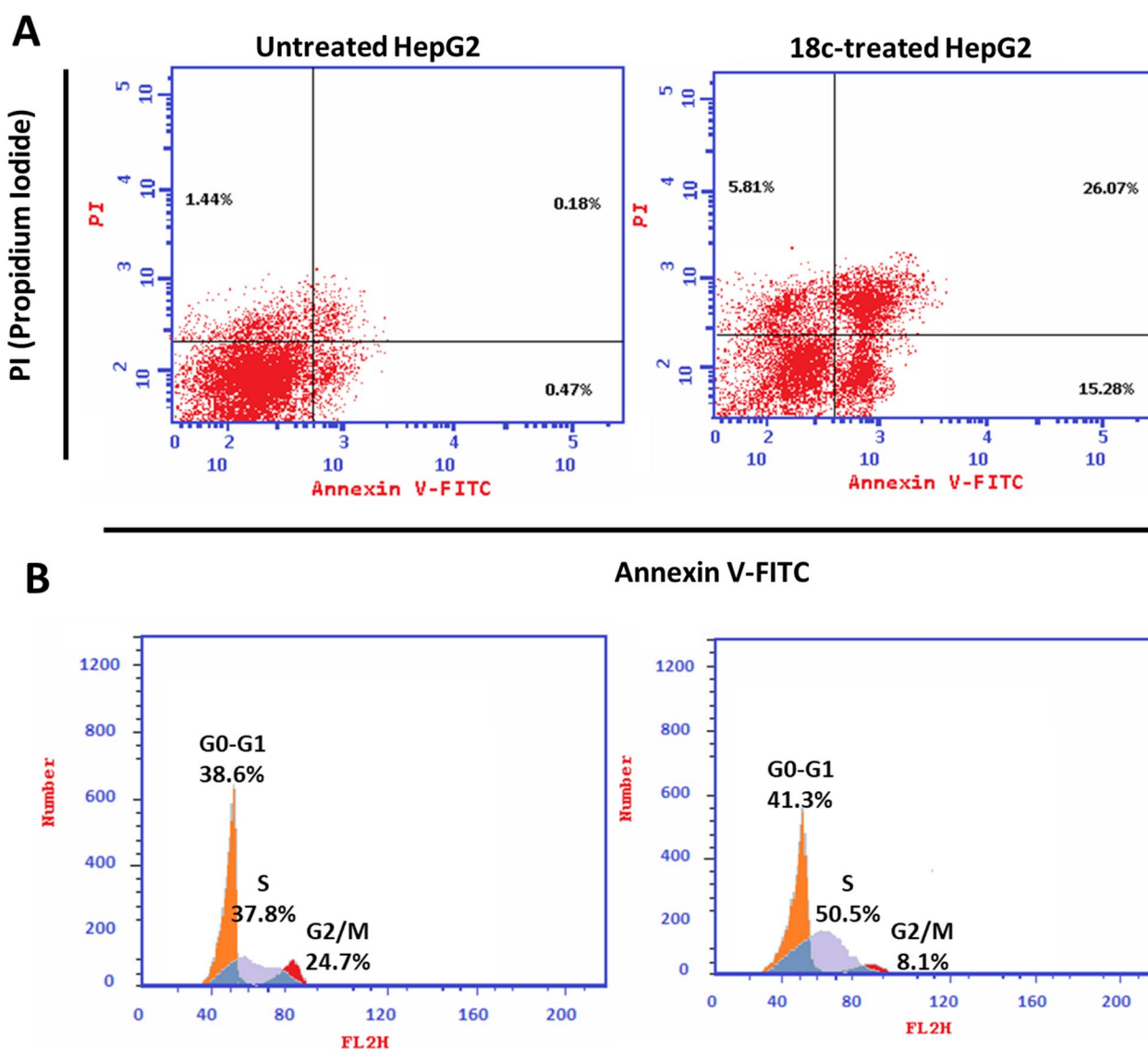


Fig. 7 **A** Cryptographs of annexin-V/Propidium Iodide staining of untreated and **18c**-treated HepG2 cells with the IC₅₀ values, 48 h, "Q1-UL (necrosis, AV-/PI+), Q1-UR (late apoptotic cells, AV+/PI+), Q1-LL (normal cells, AV-/PI-), Q1-LR (early apoptotic cells, AV+/PI-)", **B** Percentage of cell population at each cell cycle "G0-G1, S, G2/M" using flow cytometry

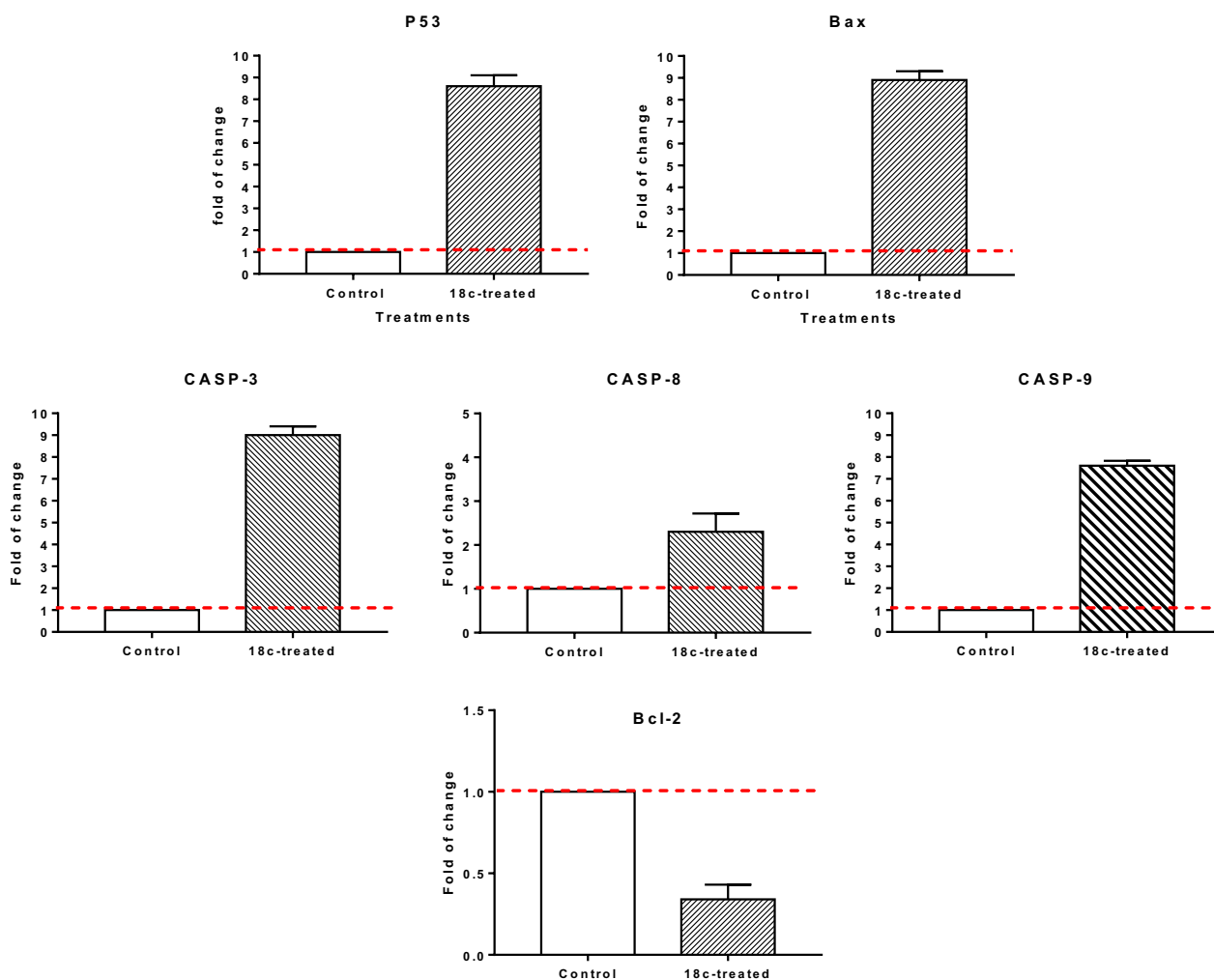


Fig. 8 Quantitative RT-PCR results analysis of the apoptosis-related genes; P53, Bax, Caspases 3, 8, 9, and Bcl-2, respectively, in HepG2 cells treated with **18c** with the IC_{50} values, 48 h. The data illustrated is the average of 3 independent experimental runs (Mean \pm SD). The red dashed line represents the fold change of control = 1

513 (M^+). Anal. Calcd. for $C_{31}H_{23}N_5OS$: C, 72.49; H, 4.51; N, 13.64; S, 6.24. Found: C, 72.44; H, 4.52; N, 13.61; S, 6.23%.

2-(4-Methoxybenzylidenehydrazinyl)-4-(4-(2-naphthoyl)-1-phenyl-pyrazol-3-yl)thiazole (8c)

Brown powder, (85% yield), mp. 121–123 °C; IR (KBr) 3408 (NH), 1600 (C=O), 1509 (C=N) cm^{-1} ; 1H -NMR: δ 3.79 (s, 3H, OCH_3), 6.97 (d, 2H, ArH, $J=8.7$), 7.39–7.66 (m, 8H, ArH), 7.89 (s, 1H, thiazole-5-H), 7.95–8.00 (m, 3H, ArH), 8.03 (s, 1H, CH=N), 8.09 (d, 2H, ArH, $J=8.4$), 8.51 (s, 1H, naphthalene-1-H), 9.01 (s, 1H, pyrazole-5-H), 11.93 (s, 1H, NH); MS: m/z 529 (M^+). Anal. Calcd. for $C_{31}H_{23}N_5O_2S$: C, 70.30; H, 4.38; N, 13.22; S, 6.05. Found: C, 70.27; H, 4.35; N, 13.24; S, 6.03%.

2-(4-Nitrobenzylidenehydrazinyl)-4-(4-(2-naphthoyl)-1-phenyl-pyrazol-3-yl)thiazole (8d)

Red powder, (81% yield), mp. 231–233 °C; IR (KBr) 3430 (NH), 1643 (C=O), 1547 (C=N) cm^{-1} ; 1H -NMR: δ 7.54 (d, 2H, ArH, $J=9.3$), 7.58–7.87 (m, 8H, ArH), 7.98 (s, 1H, thiazole-5-H), 8.01–8.04 (m, 3H, ArH), 8.05 (s, 1H, CH=N), 8.24 (d, 2H, ArH, $J=9$), 8.52 (s, 1H, naphthalene-1-H), 9.03 (s, 1H, pyrazole-5-H), 12.48 (s, 1H, NH); ^{13}C NMR: δ 109.2, 119.1, 120.9, 124.1, 124.7, 126.8, 126.9, 127.2, 127.6, 128.2, 128.6, 129.1, 129.6, 129.8, 131.6, 132.1, 132.8, 134.9, 135.6, 138.6, 138.9, 140.8, 147.0, 147.7, 167.2, 188.9; MS: m/z 544 (M^+). Anal. Calcd. for $C_{30}H_{20}N_6O_3S$: C, 66.16; H, 3.70; N, 15.43; S, 5.89. Found: C, 66.15; H, 3.67; N, 15.41; S, 5.87%.

Synthesis of arylidenehydrazinyl-(1H-pyrazol-3-yl)thiazole derivatives 12–14

General procedure To a solution of 3-bromoacetyl-4-(2-naphthoyl)-1-phenyl-1H-pyrazole **6** (1 mmol) in ethanol (25 mL) containing triethylamine (0.2 ml), the appropriate heterocyclic-thiosemicarbazone derivatives **9–11** (1 mmol) was added. The reaction mixture was heated at reflux for 5 h and then left to cool to room temperature. The obtained solid products were filtered off, then recrystallized from ethanol/DMF to afford the 2-(ethylidenehydrazinyl)-4-(4-(2-naphthoyl)-1-phenylpyrazol-3-yl)thiazole derivatives **12–14**.

2-(2-(1-(Benzofuran-2-yl)ethylidene)hydrazinyl)-4-(4-(2-naphthoyl)-1-phenylpyrazol-3-yl)thiazole (12)

Brown powder, (85% yield), mp. 164–166 °C; IR (KBr) 3433 (NH), 1648 (C=O), 1539 (C=N) cm^{-1} ; $^1\text{H-NMR}$: δ 2.31 (s, 3H, CH_3), 7.22 (s, 1H, benzofuran-3-H), 7.25–7.67 (m, 9H, ArH), 7.89 (s, 1H, thiazole-5-H), 7.93–8.07 (m, 4H, ArH), 8.14 (d, 2H, ArH, $J=7.8$), 8.55 (s, 1H, naphthalene-1-H), 9.04 (s, 1H, pyrazole-5-H), 11.59 (s, 1H, NH); $^{13}\text{C NMR}$: δ 17.0, 103.4, 117.6, 118.4, 118.9, 119.3, 119.8, 125.9, 126.8, 127.7, 127.9, 128.5, 128.8, 129.1, 129.3, 129.6, 130.0, 130.2, 131.2, 131.1, 142.5, 151.6, 153.0, 154.1, 155.2, 158.4, 159.9, 160.3, 172.2, 188.0. MS: m/z 553 (M^+). Anal. Calcd. for $\text{C}_{33}\text{H}_{23}\text{N}_5\text{O}_2\text{S}$: C, 71.59; H, 4.19; N, 12.65; S, 5.79. Found: C, 71.56; H, 4.18; N, 12.63; S, 5.77%.

2-(2-(1-(Benzothiazol-2-yl)ethylidene)hydrazinyl)-4-(4-(2-naphthoyl)-1-phenylpyrazol-3-yl)-thiazole (13)

Creamy powder, (87% yield), mp. 143–145 °C; IR (KBr) 3410 (NH), 1635 (C=O), 1543 (C=N) cm^{-1} ; $^1\text{H-NMR}$: δ 2.45 (s, 3H, CH_3), 7.36 (s, 1H, thiazole-5-H), 7.39–8.06 (m, 13H, ArH), 8.12 (d, 2H, ArH, $J=8.1$), 8.55 (s, 1H, naphthalene-1-H), 9.04 (s, 1H, pyrazole-5-H), 12.04 (s, 1H, NH); $^{13}\text{C NMR}$: δ 13.3, 110.2, 119.1, 120.7, 122.1, 122.9, 124.8, 125.8, 126.2, 126.8, 127.3, 127.6, 128.2, 128.5, 129.6, 129.8, 131.7, 132.1, 133.5, 134.9, 135.0, 135.7, 138.9, 153.2, 168.1, 188.8; MS: m/z 570 (M^+). Anal. Calcd. for $\text{C}_{32}\text{H}_{22}\text{N}_6\text{OS}_2$: C, 67.35; H, 3.89; N, 14.73; S, 11.24. Found: C, 67.34; H, 3.86; N, 14.75; S, 11.23%.

2-(2-(1-(Coumarin-3-yl)ethylidene)hydrazinyl)-4-(4-(2-naphthoyl)-1-phenylpyrazol-3-yl)-thiazole (14)

Yellow powder, (73% yield), mp. 239–241 °C; IR (KBr) 3448 (NH), 1635 (C=O), 1519 (C=N) cm^{-1} ; $^1\text{H-NMR}$: δ 2.23 (s, 3H, CH_3), 7.34–8.14 (m, 17H, ArH, thiazole-5-H and chromen-4-H), 8.53 (s, 1H, naphthalene-1-H), 9.03 (s, 1H, pyrazole-5-H), 11.39 (s, 1H, NH); MS: m/z 581 (M^+). Anal. Calcd. for $\text{C}_{34}\text{H}_{23}\text{N}_5\text{O}_3\text{S}$: C, 70.21; H, 3.99; N, 12.04; S, 5.51. Found: C, 70.20; H, 3.96; N, 12.03; S, 5.53%.

Synthesis

of bis((2-(4-((2-naphthoyl)-1-phenyl-1H-pyrazol-3-yl)thiazol-2-yl)hydrazono)-methyl)phenoxy)alkanes 18a-c and 21a-c

General procedure To a mixture of the appropriate 4,4'-(alkane-diylbis(oxy))dibenzaldehydethiosemicarbazone derivatives **17a-c** or 2,2'-(alkane-diylbis(oxy))dibenzaldehydethiosemicarbazone derivatives **19a-c** (1.0 mmol) and 3-bromoacetyl-4-(2-naphthoyl)-1-phenyl-1H-pyrazole (**6**) (2.0 mmol) in ethanol (25 mL), triethylamine (0.2 mL) were added. The reaction mixture was heated under reflux temperature for 4–6 h and then allowed to cool to room temperature. The solvent was then evaporated under vacuum, and the solid residue was collected by filtration and recrystallized from ethanol/DMF to give the corresponding bis-pyrazolythiazoles **18a-c** and **21a-c**.

1,2-Bis(4-((2-(4-((2-naphthoyl)-1-phenyl-1H-pyrazol-3-yl)thiazol-2-yl)hydrazono)methyl)-phenoxy)ethane (18a)

Off-white powder, (79% yield), mp. 187–189 °C; IR (KBr) 3407 (NH), 1645 (C=O), 1505 (C=N) cm^{-1} ; $^1\text{H-NMR}$: δ 4.35 (s, 4H, CH_2O), 7.03 (d, 4H, ArH, $J=7.8$), 7.36–7.68 (m, 16H, ArH), 7.91 (s, 2H, thiazole-5-H), 7.98–8.02 (m, 6H, ArH), 8.06 (s, 2H, $\text{CH}=\text{N}$), 8.11 (d, 4H, ArH, $J=7.8$), 8.51 (s, 2H, naphthalene-1-H), 9.01 (s, 2H, pyrazole-5-H), 11.90 (s, 2H, NH); $^{13}\text{C NMR}$: δ 66.4, 108.1, 114.8, 119.0, 120.9, 124.7, 126.8, 127.1, 127.2, 127.6, 127.7, 128.2, 128.5, 128.9, 129.6, 129.8, 131.6, 132.1, 132.7, 134.9, 135.7, 138.9, 141.1, 148.0, 159.2, 167.7, 189.0; MS: m/z 529 ($\text{M}^+/2$). Anal. Calcd. for $\text{C}_{62}\text{H}_{44}\text{N}_{10}\text{O}_4\text{S}_2$: C, 70.44; H, 4.19; N, 13.25; S, 6.07. Found: C, 70.45; H, 4.17; N, 13.25; S, 6.06%.

1,3-Bis(4-((2-(4-((2-naphthoyl)-1-phenyl-1H-pyrazol-3-yl)thiazol-2-yl)hydrazono)methyl)-phenoxy)propane (18b)

Off-white powder, (80% yield), mp. 200–202 °C; IR (KBr) 3431 (NH), 1634 (C=O), 1508 (C=N) cm^{-1} ; $^1\text{H-NMR}$: δ 2.21 (m, 2H, CH_2), 4.17 (m, 4H, CH_2O), 6.99 (d, 4H, ArH, $J=8.1$), 7.39–7.65 (m, 16H, ArH), 7.89 (s, 2H, thiazole-5-H), 7.98 (m, 6H, ArH), 8.05 (s, 2H, $\text{CH}=\text{N}$), 8.11 (d, 4H, ArH, $J=7.8$), 8.50 (s, 2H, naphthalene-1-H), 9.01 (s, 2H, pyrazole-5-H), 11.95 (s, 2H, NH); $^{13}\text{C NMR}$: δ 27.4, 67.0, 103.4, 109.1, 114.5, 118.5, 119.9, 121.2, 127.3, 128.6, 128.7, 129.0, 129.1, 129.5, 129.6, 130.2, 133.7, 136.2, 137.2, 137.4, 148.9, 149.9, 157.2, 160.2, 162.0, 166.4, 189.9; MS: m/z 529 ($\text{M}^+/2$). Anal. Calcd. for $\text{C}_{63}\text{H}_{46}\text{N}_{10}\text{O}_4\text{S}_2$: C, 70.64; H, 4.33; N, 13.08; S, 5.99. Found: C, 70.63; H, 4.30; N, 13.07; S, 5.97%.

1,4-Bis(4-((2-(4-((2-naphthoyl)-1-phenyl-1H-pyrazol-3-yl)thiazol-2-yl)hydrazono)methyl)-phenoxy)butane (18c)

Off-white powder, (83% yield), mp. 223–225 °C; IR (KBr) 3435 (NH), 1647 (C=O), 1566 (C=N) cm^{-1} ; $^1\text{H-NMR}$: δ 2.24 (m, 4H, CH_2), 4.36 (m, 4H, CH_2O), 7.02 (d, 4H, ArH, $J=7.5$), 7.39–7.70(m, 16H, ArH), 7.87–7.91 (m, 8H, thiazole-5-H, ArH), 7.98 (s, 2H, $\text{CH}=\text{N}$), 8.13 (d, 4H, ArH, $J=6.9$), 8.53 (s, 2H, naphthalene-1-H), 9.02 (s, 2H, pyrazole-5-H), 11.11 (s, 2H, NH); MS: m/z 543 ($\text{M}^+/2$). Anal. Calcd. For $\text{C}_{64}\text{H}_{48}\text{N}_{10}\text{O}_4\text{S}_2$: C, 70.83; H, 4.46; N, 12.91; S, 5.91. Found: C, 70.81; H, 4.45; N, 12.91; S, 5.90.

1,2-Bis(2-((2-(4-((2-naphthoyl)-1-phenyl-1H-pyrazol-3-yl)thiazol-2-yl)hydrazono)methyl)-phenoxy)ethane (20a)

Off-white powder, (71% yield), mp. 166–168 °C; IR (KBr) 3432 (NH), 1645 (C=O), 1571 (C=N) cm^{-1} ; $^1\text{H-NMR}$: δ 4.40 (s, 4H, CH_2O), 7.13 (d, 4H, ArH, $J=7.5$), 7.36–7.77 (m, 16H, ArH), 7.95 (s, 2H, thiazole-5-H), 7.98 (m, 6H, ArH), 8.06 (d, 4H, ArH, $J=8.7$), 8.29 (s, 2H, $\text{CH}=\text{N}$), 8.45 (s, 2H, naphthalene-1-H), 8.99 (s, 2H, pyrazole-5-H), 11.99 (s, 2H, NH); $^{13}\text{C NMR}$: δ 67.7, 102.1, 109.1, 112.1, 115.1, 116.7, 117.0, 119.8, 121.0, 124.8, 127.3, 127.6, 127.7, 129.1, 129.3, 131.7, 135.4, 136.4, 138.7, 139.2, 141.0, 144.0, 153.4, 156.4, 162.2, 148.0, 170.1, 192.0; MS: m/z 529 ($\text{M}^+/2$) Anal. Calcd. for $\text{C}_{62}\text{H}_{44}\text{N}_{10}\text{O}_4\text{S}_2$: C, 70.44; H, 4.19; N, 13.25; S, 6.07. Found: C, 70.45; H, 4.17; N, 13.25; S, 6.06%.

1,3-Bis(2-((2-(4-((2-naphthoyl)-1-phenyl-1H-pyrazol-3-yl)thiazol-2-yl)hydrazono)methyl)-phenoxy)propane (20b)

Off-white powder, (75% yield), mp. 209–211 °C; IR (KBr) 3429 (NH), 1645 (C=O), 1573 (C=N) cm^{-1} ; $^1\text{H-NMR}$: δ 2.22 (m, 2H, CH_2), 4.24(m, 4H, CH_2O), 7.08 (d, 4H, ArH, $J=6.6$), 7.29–7.75 (m, 16H, ArH), 7.90 (s, 2H, thiazole-5-H), 7.98–8.06 (m, 6H, ArH), 8.11 (d, 4H, ArH, $J=7.5$), 8.33 (s, 2H, $\text{CH}=\text{N}$), 8.50 (s, 2H, naphthalene-1-H), 9.01 (s, 2H, pyrazole-5-H), 11.99 (s, 2H, NH); MS: m/z 529 ($\text{M}^+/2$). Anal. Calcd. for $\text{C}_{63}\text{H}_{46}\text{N}_{10}\text{O}_4\text{S}_2$: C, 70.64; H, 4.33; N, 13.08; S, 5.99. Found: C, 70.63; H, 4.30; N, 13.07; S, 5.97%.

1,4-Bis(2-((2-(4-((2-naphthoyl)-1-phenyl-1H-pyrazol-3-yl)thiazol-2-yl)hydrazono)methyl)-phenoxy)butane (20c)

Off-white powder, (84% yield), mp. 230–232 °C; IR (KBr) 3439 (NH), 1601 (C=O), 1507 (C=N) cm^{-1} ; $^1\text{H-NMR}$: δ 1.94 (m, 4H, CH_2), 4.09 (m, 4H, CH_2O), 7.04(d, 4H, ArH, $J=8.1$), 7.32–7.75 (m, 16H, ArH), 7.97 (s, 2H, thiazole-5-H), 7.99 (m, 6H, ArH), 8.08 (d, 4H, ArH, $J=7.5$), 8.34 (s, 2H, $\text{CH}=\text{N}$), 8.49 (s, 2H, naphthalene-1-H), 9.00 (s, 2H, pyrazole-5-H), 12.02 (s, 2H, NH); MS:

m/z 543 ($\text{M}^+/2$). Anal. Calcd. for $\text{C}_{64}\text{H}_{48}\text{N}_{10}\text{O}_4\text{S}_2$: C, 70.83; H, 4.46; N, 12.91; S, 5.91. Found: C, 70.81; H, 4.45; N, 12.91; S, 5.90.

Biological part

Cytotoxicity

HepG2 liver cancer cells and THLE2 normal liver cells were bought from the National Research Institute in Egypt and cultured in “RPMI-1640” media containing L-Glutamine (Lonza Verviers SPRL, Belgium, cat#12-604F). Fetal bovine serum (Sigma-Aldrich, MO, USA) and penicillin–streptomycin at a concentration of 10% and 1%, respectively, were added to both cell lines (Lonza, Belgium). All cells were incubated following routine tissue culture work. Cells were treated with the compounds at (0.01, 0.1, 1, 10, and 100 μM) concentrations. Cell viability was assessed after 48 h using MTT solution (Promega, USA) [68]. Finally, Absorbance was subsequently measured (at 570 nm) using ELISA microplate reader (BIO-RAD, model iMark, Japan). The percentage of cell viability was calculated, and IC_{50} values were recorded using the GraphPad prism 7, as previously reported in the literature [69, 70].

EGFR and HER2 kinase inhibitory assay

Anti-EGFR and anti-HER2 activities were measured using EGFR Kinase Assay Kit “BPS Bioscience kit, Cat#40321” and HER2 Kinase Assay Kit “BPS Bioscience kit, Cat# 40721”. Kinase inhibitory assays were performed to evaluate the inhibitory potency of compounds **18b**, **18c**, and **21a** against the EGFR and HER2. The autophosphorylation percentage inhibition of compounds was calculated by: $100 - \left[\frac{\text{A}_{\text{control}}}{\text{A}_{\text{treated}}} - \text{Control} \right]$. GraphPad prism7 was used to determine IC_{50} from percent inhibition curves at five doses of each compound [71].

Investigation of apoptosis

Annexin V/PI staining and cell cycle analysis Overnight, 6-well culture plates were stocked with HepG2 cells ($3-5 \times 10^5$ cells/well). After determining the IC_{50} values, cells were treated with compound **18c** for 48 h. After that, the cells and the medium supernatants were separated and washed with ice-cold PBS. The next step was suspending the cells in 100 μL of annexin binding buffer solution “25 mM CaCl_2 , 1.4 M NaCl, and 0.1 M HEPES/NaOH, pH 7.4” and incubation with “Annexin V-FITC solution (1:100) and propidium iodide (PI)” at a concentration equals 10 $\mu\text{g}/\text{mL}$ in the dark for 30 min. After the cells were stained, they were gathered by Cytoflex FACS equipment. We used cytExpert to examine the data [72–74].

Real-time-polymerase chain reaction for the selected genes Genes of P53, Bax, and Caspases-3,8,9 were screened as proapoptotic genes, while Bcl-2 was screened as antiapoptotic, therefore, we measured their gene expression to investigate the apoptotic process. HepG2 cells were then treated with compound **18c** at their IC_{50} values for 48 h. After treatment, RT-PCR reaction was carried out following routine work. The Ct values were then used to determine the fold change in gene expression between samples after normalization to the β -actin reference gene [72, 75].

Conclusions

In this article, we introduced 2-naphthoyl moiety into the 3-position of the pyrazolyl-thiazole backbone to generate novel combined naphthalene-pyrazole-aminothiazole hybrids as simple and bis-forms. The results revealed that some of the obtained molecular hybrids had remarkable potential as anti-cancer agents. Investigating the cytotoxicity, compound **18c** showed potent cytotoxicity with an IC_{50} value of 0.97 μ M compared to Lapatinib (IC_{50} = 7.45 μ M). Additionally, they were safe (non-cytotoxic) against the THLE2 cells. Compounds **18c** exhibited promising EGFR/HER2 inhibitory activities with IC_{50} values of 4.98 and 9.85 nM, respectively, compared to Lapatinib (IC_{50} = 6.1 and 17.2 nM). Compound **18c** significantly activated liver apoptotic cell death, increasing the death rate by 63.6-fold and arresting cell proliferation at S-phase. Additionally, compound **18c** affected the apoptosis-related genes by upregulating the proapoptotic and downregulating the antiapoptotic gene. Thereby compound **18c** exhibited promising cytotoxicity against HepG2 cells through EGFR/HER2 inhibition. Interestingly, doubling the molecular hybrids in the form of bis-heterocycles led to an extraordinary improvement in the cytotoxic efficiency compared with the simple molecular hybrids, where doubling the pharmacophoric scaffold led to about an eightfold increase in the cytotoxic potency (IC_{50} = 0.97 μ M for **18c** vs. 7.39 μ M for **8c**).

Abbreviations

EGFR	Epidermal growth factor receptor
HER2	Human epidermal growth factor receptor 2
RT-PCR	Reverse transcription polymerase chain reaction (RT-PCR)
$\Delta\Psi$ m	Mitochondrial potential; Bcl-2: B-cell lymphoma 2
Bax	Bcl-2-associated X protein
SD	Standard deviation
IC_{50}	Half-maximal inhibitory concentration
NSCLC	Non-small cell lung carcinoma;
HepG2	Liver cancer cells
THLE2	Normal liver cells
G2/M, S, G1, G0	Cell cycle phases

Supplementary Information

The online version contains supplementary material available at <https://doi.org/10.1186/s13065-023-00921-6>.

Additional file 1: Figure S1. 1H NMR spectrum of compound 6. **Figure S2.** 1H NMR spectrum of compound 8a. **Figure S3.** 13C NMR spectrum of compound 8a. **Figure S4.** 1H NMR spectrum of compound 8b. **Figure S5.** 13C NMR spectrum of compound 8b. **Figure S6.** 1H NMR spectrum of compound 8c. **Figure S7.** 1H NMR spectrum of compound 8d. **Figure S8.** 13C NMR spectrum of compound 8d. **Figure S9.** 1H NMR spectrum of compound 12. **Figure S10.** 13CNMR spectrum of compound 12. **Figure S11.** 1H NMR spectrum of compound 13. **Figure S12.** 13C NMR spectrum of compound 13. **Figure S13.** 1H NMR spectrum of compound 14. **Figure S14.** 1H NMR spectrum of compound 18a. **Figure S15.** 13C NMR spectrum of compound 18a. **Figure S16.** 1H NMR spectrum of compound 18b. **Figure S17.** 13C NMR spectrum of compound 18b. **Figure S18.** 1H NMR spectrum of compound 18c. **Figure S19.** 1HNMR spectrum of compound 20a. **Figure S20.** 13C NMR spectrum of compound 20a. **Figure S21.** 1H NMR spectrum of compound 20b. **Figure S22.** 1H NMR spectrum of compound 20c. **Figure S23.** IR spectrum of compound 8a. **Figure S24.** Mass spectrum of compound 8a. **Figure S25.** IR spectrum of compound 8b. **Figure S26.** Mass spectrum of compound 8b. **Figure S27.** IR spectrum of compound 8c. **Figure S28.** Mass spectrum of compound 8c. **Figure S29.** IR spectrum of compound 12. **Figure S30.** Mass spectrum of compound 12. **Figure S31.** IR spectrum of compound 13. **Figure S32.** Mass spectrum of compound 13. **Figure S33.** IR spectrum of compound 14. **Figure S34.** Mass spectrum of compound 14. **Figure S35.** IR spectrum of compound 18b. **Figure S36.** Mass spectrum of compound 18b. **Figure S37.** IR spectrum of compound 18c. **Figure S38.** Mass spectrum of compound 18c. **Figure S39.** IR spectrum of compound 20a. **Figure S40.** Mass spectrum of compound 20a. **Figure S41.** IR spectrum of compound 20b. **Figure S42.** Mass spectrum of compound 20b. **Figure S43.** IR spectrum of compound 20c. **Figure S44.** Mass spectrum of compound 20c.

Acknowledgements

Not applicable

Author contributions

MES, EAR, and KMD designed the idea of synthetic organic chemistry, and made formal analyses of characterization charts, MES, and EMM synthesized the compounds under the supervision of KMD. In addition, MSN designed the concept and carried out the biological analyses. All authors contributed to writing the manuscript with their corresponding parts and agreed to the final manuscript form. All authors read and approved the final manuscript.

Funding

Not applicable.

Availability of data and materials

All data and analyses are available from the corresponding author on reasonable request.

Declarations

Ethics approval and consent to participate

Not applicable.

Consent for publication

Not applicable.

Competing interests

The authors declare that they have no competing interests.

Received: 19 November 2022 Accepted: 23 February 2023
Published online: 08 June 2023

References

- Makar S, Saha T, Singh SK. Naphthalene, a versatile platform in medicinal chemistry: sky-high perspective. *Eur J Med Chem.* 2019;161:252–76.
- Unzner TA, Grossmann AS, Magauer T. Rapid access to orthogonally functionalized naphthalenes: application to the total synthesis of the anti-cancer agent chartarin. *Angew Chem Int Ed.* 2016;55:9763–7.
- Valente S, Trisciuglio D, De Luca T, Nebbioso A, et al. 1,3,4-Oxadiazole-containing histone deacetylase inhibitors: anti-cancer activities in cancer cells. *J Med Chem.* 2014;57:6259–65.
- Wang G, Peng Z, Zhang J, Qiu J, et al. Synthesis, biological evaluation and molecular docking studies of aminochalcone derivatives as potential anti-cancer agents by targeting tubulin colchicine binding site. *Bioorg Chem.* 2018;78:332–40.
- Wang G, Liu W, Gong Z, Huang Y, et al. Synthesis, biological evaluation, and molecular modelling of new naphthalene-chalcone derivatives as potential anti-cancer agents on MCF-7 breast cancer cells by targeting tubulin colchicine binding site. *J Enz Inhib Med Chem.* 2020;35:139–44.
- Wang G, Liu W, Tang J, et al. Design, synthesis, and anti-cancer evaluation of benzophenone derivatives bearing naphthalene moiety as novel tubulin polymerization inhibitors. *Bioorg Chem.* 2020;104: 104265.
- Wang G, Qiu J, Xiao X, et al. Synthesis, biological evaluation and molecular docking studies of a new series of chalcones containing naphthalene moiety as anti-cancer agents. *Bioorg Chem.* 2018;76:249–57.
- Fukamiya N, Lee KH. Antitumor agents, 81 justicidin-a and diphyllin, two cytotoxic principles from *Justicia procumbens*. *J Nat Prod.* 1986;49:348–50.
- Xia L, Idhayadhulla A, Lee YR, Kim SH, Wee YJ. Antioxidant and antibacterial evaluation of synthetic furomollugin and its diverse analogs. *Med Chem Res.* 2014;23:3528–38.
- Ibrahim SR, Mohamed GA. Naturally occurring naphthalenes: chemistry, biosynthesis, structural elucidation, and biological activities. *Phytochem Rev.* 2016;15:279–95.
- Abozeid MA, El-Sawi AA, Abdelmoteleb M, Awad H, et al. Synthesis of novel naphthalene-heterocycle hybrids with potent antitumor, anti-inflammatory and antituberculosis activities. *RSC Adv.* 2020;10:42998–42009.
- Saif MW, Oettle H, Vervenne WL, Thomas JP, et al. Randomized double-blind phase II trial comparing gemcitabine plus LY293111 versus gemcitabine plus placebo in advanced adenocarcinoma of the pancreas. *Cancer J.* 2009;15:339–43.
- Jänne PA, Paz-Ares L, Oh Y, Eschbach C, et al. Randomized, double-blind, phase II trial comparing gemcitabine-cisplatin plus the LTB4 antagonist LY293111 versus gemcitabine-cisplatin plus placebo in first-line non-small-cell lung cancer. *J Thorac Oncol.* 2014;9:126–31.
- Sharma PC, Bansal KK, Sharma A, Sharma D, Deep A. Thiazole-containing compounds as therapeutic targets for cancer therapy. *Eur J Med Chem.* 2020;188: 112016.
- Petrou A, Fesatidou M, Geronikaki A. Thiazole ring a biologically active scaffold. *Molecules.* 2021;26:3166.
- Ayati A, Emami S, Moghimi S, Foroumadi A. Thiazole in the targeted anti-cancer drug discovery. *Future Med Chem.* 2019;11:1929–52.
- Chhabria TM, Patel S, Modi P, Brahmshatriya PS. Thiazole: a review on chemistry, synthesis and therapeutic importance of its derivatives. *Curr Top Med Chem.* 2016;16:2841–62.
- Leoni A, Locatelli A, Morigi R, Rambaldi M. Novel thiazole derivatives: a patent review (2008–2012 Part 2). *Expert Opin Therap Pat.* 2014;24:759–77.
- Franchetti P, Cappellacci L, Grifantini M, Barzi A, et al. Furanfuran and thiophenfurin: two novel tiazofurin analogs synthesis, structure, antitumor activity, and interactions with inosine monophosphate dehydrogenase. *J Med Chem.* 1995;38:3829–37.
- Li X, He Y, Ruiz CH, Koenig M, Cameron MD. Characterization of dasatinib and its structural analogs as CYP3A4 mechanism-based inactivators and the proposed bioactivation pathways. *Drug Metab Dispos.* 2009;37:1242–50.
- Hu-Lieskovan S, Mok S, Homet MB, Tsoi J, et al. Improved antitumor activity of immunotherapy with BRAF and MEK inhibitors in BRAF V600E melanoma. *Sci Transl Med.* 2015;7:279–341.
- Zhang X, Gureasko J, Shen K, Cole PA, Kuriyan J. An allosteric mechanism for activation of the kinase domain of epidermal growth factor receptor. *Cell.* 2006;125:1137–49.
- Fleming TP, Saxena A, Clark WC, Robertson JT, et al. Amplification and/or overexpression of platelet-derived growth factor receptors and epidermal growth factor receptor in human glial tumors. *Cancer Res.* 1992;52:4550–3.
- Luo Y, Li Y, Qiu KM, Lu X, et al. Metronidazole acid acyl sulfonamide: a novel class of anti-cancer agents and potential EGFR tyrosine kinase inhibitors. *Bioorg Med Chem.* 2011;19:6069–76.
- Chandregowda V, Venkateswara RG, Chandrasekara RG. Convergent approach for commercial synthesis of gefitinib and erlotinib. *Org Process Res Develop.* 2007;11:813–6.
- Qiu KM, Wang HH, Wang LM, Luo Y, et al. Design, synthesis and biological evaluation of pyrazolyl-thiazolinone derivatives as potential EGFR and HER-2 kinase inhibitors. *Bioorg Med Chem.* 2012;20:2010–8.
- Ebenezer O, Shapi M, Tuszynski JA. A review of the recent development in the synthesis and biological evaluations of pyrazole derivatives. *Biomedicines.* 2022;10:1124.
- Vujanović I, Paravić-Radičević A, Brajška K, Bertoša B. Synthesis and biological validation of novel pyrazole derivatives with anti-cancer activity guided by 3D-QSAR analysis. *Bioorg Med Chem.* 2012;20:2101–10.
- Liu DC, Gao MJ, Huo Q, Ma T, et al. Design, synthesis, and apoptosis-promoting effect evaluation of novel pyrazole with benzo [d] thiazole derivatives containing aminoguanidine units. *J Enz Inhib Med Chem.* 2019;34:829–37.
- Shaw AT, Yasothan U, Kirkpatrick P. Crizotinib. *Nat Rev Drug Disc.* 2011;10:897–8.
- Yamaguchi N, Lucena-Araujo AR, Nakayama S, de Figueiredo-Pontes LL, et al. Dual ALK and EGFR inhibition targets a mechanism of acquired resistance to the tyrosine kinase inhibitor crizotinib in ALK rearranged lung cancer. *Lung Cancer.* 2014;83:37–43.
- Kantarjian HM, Silver RT, Komrokji RS, Mesa RA, et al. Ruxolitinib for myelofibrosis—an update of its clinical effects. *Clin Lymph Myelom Leukem.* 2013;13:638–45.
- Viegas-Junior C, Danuello A, da Silva BV, Barreiro EJ, Fraga CAM. Molecular hybridization: a useful tool in the design of new drug prototypes. *Current Med Chem.* 2007;14:1829–52.
- Ivasiv V, Albertini C, Gonçalves AE, Rossi M, Bolognesi ML. Molecular hybridization as a tool for designing multitarget drug candidates for complex diseases. *Curr Top Med Chem.* 2019;19:1694–711.
- Shin SY, Ahn S, Yoon H, Jung H, et al. Colorectal anti-cancer activities of polymethoxylated 3-naphthyl-5-phenylpyrazoline-carbothioamides. *Bioorg Med Chem Lett.* 2016;26:4301–9.
- Wang G, Liu W, Peng Z, Huang Y, Gong Z, Li Y. Design, synthesis, molecular modeling, and biological evaluation of pyrazole-naphthalene derivatives as potential anti-cancer agents on MCF-7 breast cancer cells by inhibiting tubulin polymerization. *Bioorg Chem.* 2020;103:104141–9.
- Nagaraju B, Kovvuri J, Kumar CG, Routhu SR, et al. Synthesis and biological evaluation of pyrazole linked benzothiazole- β -naphthol derivatives as topoisomerase I inhibitors with DNA binding ability. *Bioorg Med Chem.* 2019;27:708–20.
- Gutierrez DA, Contreras L, Villanueva PJ, Borrego EA, et al. Identification of a potent cytotoxic pyrazole with anti-breast cancer activity that alters multiple pathways. *Cells.* 2022;11:254.
- Wang G, Liu W, Fan M, He M, et al. Design, synthesis and biological evaluation of novel thiazole-naphthalene derivatives as potential anti-cancer agents and tubulin polymerisation inhibitors. *J Enz Inhib Med Chem.* 2021;36:1693–701.
- Yuan JW, Wang SF, Luo ZL, Qiu HY, et al. Synthesis and biological evaluation of compounds which contain pyrazole, thiazole and naphthalene ring as antitumor agents. *Bioorg Med Chem Lett.* 2014;24:2324–8.
- Hegazi B, Mohamed HA, Dawood KM, Badria FAR. Cytotoxicity and utility of 1-indanone in the synthesis of some new heterocycles. *Chem Pharm Bull.* 2010;58:479–83.
- Abdel-Aziz HA, El-Zahabi HS, Dawood KM. Microwave-assisted synthesis and in-vitro anti-tumor activity of 1, 3, 4-triaryl-5-N-arylpyrazole-carboxamides. *Eur J Med Chem.* 2010;45:2427–32.
- Dawood KM, Abdel-Gawad H, Mohamed HA, Badria FA. Synthesis, anti-HSV-1, and cytotoxic activities of some new pyrazole-and isoxazole-based heterocycles. *Med Chem Res.* 2011;20:912–9.
- Dawood KM, Eldebss TM, El-Zahabi HS, Yousef MH, Metz P. Synthesis of some new pyrazole-based 1, 3-thiazoles and 1, 3, 4-thiadiazoles as anti-cancer agents. *Eur J Med Chem.* 2013;70:740–9.

45. Farghaly TA, Abbas EM, Dawood KM, El-Naggar TB. Synthesis of 2-phenylazonaphtho [1,8-ef][1,4]diazepines and 9-(3-arylhydrazono)pyrrolo[1,2-a]perimidines as antitumor agents. *Molecules*. 2014;19:740–55.
46. Dawood KM, Gomha SM. Synthesis and anti-cancer activity of 1,3,4-thiadiazole and 1,3-thiazole derivatives having 1,3,4-oxadiazole moiety. *J Heterocycl Chem*. 2015;52:1400–5.
47. Behbehani H, Aryan FA, Dawood KM, Ibrahim HM. High pressure assisted synthetic approach for novel 6,7-dihydro-5H-benzo[6,7]cyclohepta[1,2-b]pyridine and 5,6-dihydrobenzo[h]quinoline derivatives and their assessment as anti-cancer agents. *Sci Rep*. 2020;10:1–17.
48. Dawood KM, Raslan MA, Abbas AA, Mohamed BE, et al. Novel Bis-thiazole derivatives: synthesis and potential cytotoxic activity through apoptosis with molecular docking approaches. *Front Chem*. 2021;9: 694870.
49. Thabet FM, Dawood KM, Ragab EA, Nafie MS, Abbas AA. Design and synthesis of new bis(1,2,4-triazolo[3,4-b][1,3,4]thiadiazines) and bis(quinoxalin-2-yl)phenoxy)alkanes as anti-breast cancer agents through dual PARP-1 and EGFR targets inhibition. *RSC Adv*. 2022;12:23644–60.
50. Dawood KM, Raslan MA, Abbas AA, Mohamed BE, Nafie MS. Novel bis-amide-based bis-thiazoles as anti-colorectal cancer agents through Bcl-2 inhibition: synthesis, in vitro, and in vivo studies. *Anti-cancer Agents Med Chem*. 2023;23:328–45.
51. Abbas AA, Dawood KM. Benzofuran scaffolds as promising anticancer agents. *RSC Adv*. 2023;13:11096–120.
52. Lv PC, Li DD, Li QS, Lu X, et al. Synthesis, molecular docking and evaluation of thiazolyl-pyrazoline derivatives as EGFR TK inhibitors and potential anti-cancer agents. *Bioorg Med Chem Lett*. 2011;21:5374–7.
53. Sever B, Altıntop MD, Radwan MO, Özdemir A, et al. Design, synthesis and biological evaluation of a new series of thiazolyl-pyrazolines as dual EGFR and HER2 inhibitors. *Eur J Med Chem*. 2019;182: 111648.
54. Sabry MA, Ghaly MA, Maarouf AR, El-Subbagh HI. New thiazole-based derivatives as EGFR/HER2 and DHFR inhibitors: synthesis, molecular modeling simulations and anti-cancer activity. *Eur J Med Chem*. 2022;241: 114661.
55. Al-Saleh B, Abdelkhalik MM, Eltouky AM, Elnagdi MH. Enaminones in heterocyclic synthesis: a new regioselective synthesis of 2,3,6-trisubstituted pyridines, 6-substituted-3-arylpyridines and 1,3,5-triaroylbenzenes. *J Heterocycl Chem*. 2002;39:1035–8.
56. Dieckmann W, Platz O. Convenient synthesis of azolopyrimidine, azolo-triazine, azinobenzimidazole and 1,3,4-thiadiazole derivatives. *Chem Ber*. 1906;38:2989–95.
57. Jain SK, Mishra P. Synthesis of some 2-amino-5-Aryl-1,3,4-thiadiazoles. *Asian J Chem*. 2000;12:1341.
58. Aslam MAS, Mahmood S, Shahid M, Saeed A, Iqbal J. Synthesis, biological assay in vitro and molecular docking studies of new Schiff base derivatives as potential urease inhibitors. *Eur J Med Chem*. 2011;46:5473–9.
59. Salem ME, Darweesh AF, Elwahy AHM. Synthesis of novel scaffolds based on thiazole or triazolothiadiazine linked to benzofuran or benzothiazole moieties as new hybrid molecules. *Synth Commun*. 2020;50:256–70.
60. Somogyi L. Synthesis and transformation of 3-coumarinyl methyl ketone (thio)acylhydrazones and 5-substituted 3-acetyl-2-(3-coumarinyl)-2-methyl-1,3,4-oxadiazolines under acetylating conditions. *Liebig Annal Chem*. 1994;6:623–727.
61. Yusuf M, Jain P. Synthesis of some alkoxy based bis[thiadiazoline] derivatives. *Arab J Chem*. 2012;5:93–8.
62. Salem ME, Darweesh AF, Mekky AEM, Farag AM, Elwahy AHM. 2-Bromo-1-(1H-pyrazol-4-yl)ethanone: versatile precursor for novel mono- and bis[pyrazolylthiazoles]. *J Heterocycl Chem*. 2017;54:226–34.
63. Hosny M, Salem ME, Darweesh AF, Elwahy AHM. Synthesis of novel bis(thiazolylchromen-2-one) derivatives linked to alkyl spacer via phenoxy group. *J Heterocycl Chem*. 2018;55:2342–8.
64. Salem ME, Hosny M, Darweesh AF, Elwahy AH. Synthesis of novel bis-and poly(aryldiazonylthiazoles). *Synth Commun*. 2019;49:2319–29.
65. Radwan IT, Elwahy AHM, Darweesh AF, Sharaky M, Bagato N, Khater HF, Salem ME. Design, synthesis, docking study, and anti-cancer evaluation of novel bis-thiazole derivatives linked to benzofuran or benzothiazole moieties as PI3k inhibitors and apoptosis inducers. *J Mol Struct*. 2022;1265: 133454.
66. Ibrahim YA, Elwahy AHM, Elkareish GMM. Synthesis of new tetrabenzo nitrogen-oxygen macrocycles containing two amide groups. *J Chem Res*. 1994;414:2321.
67. Elwahy AM, Abbas A, Ibrahim Y. Synthetic approaches towards new bisformazans and bisverdazyls. *J Chem Res*. 1998;1:184–5.
68. Mosmann T. Rapid colorimetric assay for cellular growth and survival: Application to proliferation and cytotoxicity assays. *J Immunol Methods*. 1983;65:55–63.
69. Tantawy ES, Amer AM, Mohamed EK, AbdAlla MM, Nafie MS. Synthesis, characterization of some pyrazine derivatives as anti-cancer agents: In vitro and in Silico approaches. *J Mol Struct*. 2020;1210: 128013.
70. Boraie AT, Eltamany EH, Ali IA, Gebriel SM, Nafie MS. Synthesis of new substituted pyridine derivatives as potent anti-liver cancer agents through apoptosis induction: In vitro, in vivo, and in silico integrated approaches. *Bioorg Chem*. 2021;111: 104877.
71. Hisham M, Youssif BG, Osman EEA, Hayallah AM, Abdel-Aziz M. Synthesis and biological evaluation of novel xanthine derivatives as potential apoptotic antitumor agents. *Eur J Med Chem*. 2019;176:117–28.
72. Nafie MS, Arafa K, Sedky NK, Alakhdar AA, Arafa RK. Triaryl dicationic DNA minor-groove binders with antioxidant activity display cytotoxicity and induce apoptosis in breast cancer. *Chem-Biol Interact*. 2020;324: 109087.
73. Nafie MS, Amer AM, Mohamed AK, Tantawy ES. Discovery of novel pyrazolo [3,4-b] pyridine scaffold-based derivatives as potential PIM-1 kinase inhibitors in breast cancer MCF-7 cells. *Bioorg Med Chem*. 2020;28: 115828.
74. Gad EM, Nafie MS, Eltamany EH, Hammad MS, et al. Discovery of new apoptosis-inducing agents for breast cancer based on ethyl 2-amino-4,5,6,7-tetra hydrobenzo[b]thiophene-3-carboxylate: synthesis, in vitro, and in vivo activity evaluation. *Molecules*. 2020;25:2523.
75. Nafie MS, Mahgoub S, Amer AM. Antimicrobial and antiproliferative activities of novel synthesized 6-(quinolin-2-ylthio)pyridine derivatives with molecular docking study as multi-targeted JAK2/STAT3 inhibitors. *Chem Biol Drug Des*. 2021;97:553–64.

Publisher's Note

Springer Nature remains neutral with regard to jurisdictional claims in published maps and institutional affiliations.

Ready to submit your research? Choose BMC and benefit from:

- fast, convenient online submission
- thorough peer review by experienced researchers in your field
- rapid publication on acceptance
- support for research data, including large and complex data types
- gold Open Access which fosters wider collaboration and increased citations
- maximum visibility for your research: over 100M website views per year

At BMC, research is always in progress.

Learn more biomedcentral.com/submissions

